ELSEVIER

Journal of Organometallic Chemistry 635 (2001) 37–68

Journal of Organometallic Chemistry

www.elsevier.com/locate/jorganchem

Metal–dihydrogen and σ-bond coordination: the consummate extension of the Dewar–Chatt–Duncanson model for metal–olefin π bonding

Gregory J. Kubas *

Chemistry Division, MS J514, Los Alamos National Laboratory, Los Alamos, NM 87545, USA

Received 2 April 2001; accepted 30 May 2001

Abstract

There is a marvelous analogy between the metal–olefin π bonding model first brought to light by Dewar 50 years ago and that of σ-bond coordination discovered by us 17 years ago. In some ways it is surprising that 33 years elapsed between the two parallel bonding situations. However this difference pales in comparison to that between the actual synthesis of the first olefin complex, Zeise's salt in 1837, and the first recognized dihydrogen complex nearly 150 years later. This article delineates the principles of σ-bond coordination and activation inspired by the Dewar–Chatt–Duncanson model and illuminates the often-spectacular interplay between theory and experiment in this field. Aside from H–H bond coordination and activation towards cleavage, the structure and bonding principles apply to Si–H, C–H, and virtually any two-electron X–H or X–Y bond. Metal d to σ* X–H backdonation is the key to stabilizing σ-bond coordination and is also crucial to homolytic cleavage (oxidation addition). There are some differences in bonding depending on X, and, in the case of B–H bond coordination, in metal–borane complexes, backdonation to boron p orbitals occurs. For electrophilic complexes, particularly cationic systems with minimal backdonation, heterolytic cleavage of X–H is common and is a key reaction in industrial and biological catalysis. Thus there are two separate pathways for σ-bond activation that directly depend on the electronics of the metal σ-ligand bonding.

Keywords: σ-Bond coordination; Dewar–Chatt–Duncanson model; Metal–olefin π bonding; Nonclassical bonding; Backdonation; Metal–dihydrogen complex; Metal–silane complex; Metal–borane complex; Oxidative addition; Trans-effect

1. Overview of metal–dihydrogen and σ-bond coordination and analogy to metal π-bond complexes

1.1. Historical perspectives

Our discovery in 1983 of a new type of chemical bonding, stable coordination of a nearly intact dihydrogen molecule in $W(CO)_3(P^iPr_3)_2(H_2)$, was completely unexpected and was a defining event in the historical development of coordination chemistry [1].

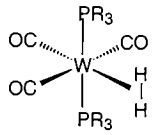

1

The H–H bond distance, d_{HH}, is stretched about 20% over its value in free H_2 (0.74 Å), but otherwise behaves as a reversibly-bound H_2 molecule much like O_2 bound to iron in hemoglobin. Metal-hydride complexes formed by oxidative addition (OA) of the H–H bond had early on been known to be a part of the catalytic hydrogenation cycle and were well-characterized species.

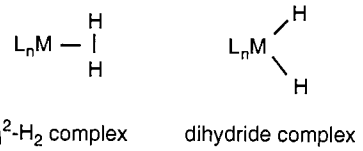

η^2-H_2 complex dihydride complex

However, the dihydrogen complexes that were only assumed to be unobservable intermediates in dihydride formation were unrecognized until our work, and indeed their isolation astounded coordination chemists at

* Tel.: +1-505-6675767; fax: +1-505-6673314.
E-mail address: kubas@lanl.gov (G.J. Kubas).

0022-328X/01/$ - see front matter
PII: S0022-328X(01)01066-X

the time. Remarkably, even the *theoretical* basis for interaction of a σ bond with a metal center was still in its infancy this late in the history of inorganic chemistry.

By 1920, Lewis developed the concept of donation of nonbonding electron pairs (lone pairs) to the metal as forming *the* coordinate bond, e.g. donation of the ammonia lone pair to Co(III) was implicated in the classical Werner $Co–NH_3$ complexes. Subsequent research extended the coordination concept beyond lone-pair donors. Around 1950, discoveries by Wilkinson, Chatt, Fischer and others showed how the π electrons of unsaturated ligands such as cyclopentadienyl and ethylene can bind to metal centers. The bonding model in such π complexes was established by Dewar in his classic paper that is being honored in this special issue, and this helped to stimulate the development of organometallic chemistry and homogeneous catalysis. The Dewar model clearly has had a major influence on the field of σ-bond coordination and activation because of the remarkably similar bonding principles, most crucially *retrodative bonding* or, as termed in this paper, *backdonation*.

Complementary to π complexes, the molecular-hydrogen complex provided the perfect archetypal example of a *sigma complex* wherein a σ-bonding electron pair (H:H) binds a ligand to a metal. This extended the coordination concept to a third (and presumably final) category: donation of a *bonding electron pair* to a vacant metal orbital.

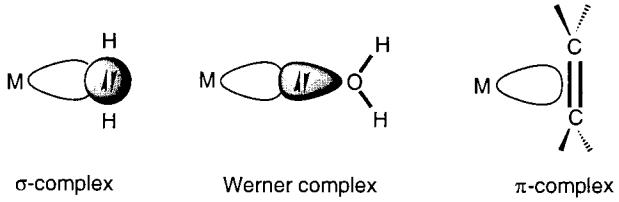

There is an interesting parallel between σ and π complexes, although the time frames between the initial

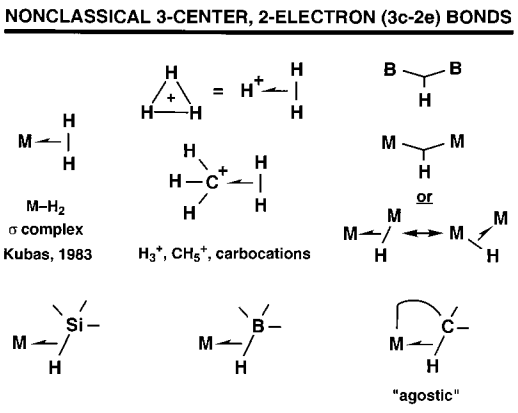

Fig. 1. Examples of nonclassical three-center, two-electron (3c–2e) bonding.

syntheses and the understanding of the structure and bonding were vastly different. The first olefin complex, Zeise's salt, $K[PtCl_3(C_2H_4)]\cdot H_2O$, was prepared in 1837 (before the periodic table was even established), while the first recognized dihydrogen complex, **1**, was not isolated until 1979, a 142 year gap! However, it took only about 4 years to establish the structure and bonding of the σ complex while about 113 years passed before the model for metal–olefin coordination was described by Dewar. Of course the structural and computational methodologies were already well developed for characterizing $M–H_2$ coordination when it was first suspected to occur in $W(CO)_3(P^iPr_3)_2(H_2)$ from infrared spectroscopic evidence [1]. Also, because H_2 is unique in containing just one pair of σ-bonding electrons, the nature of the bonding was unambiguous and more readily apparent then for π-bonding. Nonetheless, several complexes initially thought to be classical hydrides (and synthesized before **1**) were only later found to contain η^2-H_2, which shows how well hidden σ-bond coordination was even in modern times [1].

1.2. Nonclassical bonding in σ complexes compared to olefin bonding

A σ ligand is virtually always side-on bonded to the metal, and the bonding in $M–\eta^2$-H_2 and other σ-complexes has been termed *nonclassical*, on analogy to the three-center, two-electron (3c–2e) bonding in carbocations and boranes (Fig. 1). Indeed, transition metal fragments, CH_3^+, and H^+ are regarded as *isolobal* species by Hoffmann [2], possessing similar chemical bonding properties, especially towards nonclassical coordination of H_2:

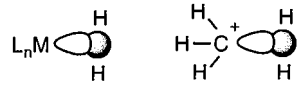

Positively-charged fragments such as $[ML_n]^+$, CH_3^+, and H^+ are all strong electrophiles towards the Lewis-basic H_2, but as will be shown, transition metals can uniquely stabilize H_2 and other σ-bond coordination. H_2 is the only σ ligand bound symmetrically; in all other cases, the $M–\eta^2$-HX bonding is asymmetric, i.e. X is farther from M than H (X = Si, B, etc.). Here there is some similarity to M–H–M, which can be viewed as a dynamic σ interaction between a metal center and M–H. The half-arrow used to represent the nonclassical bonding, as shown in Fig. 1, is now usually replaced by a line. Intramolecular agostic σ-bond interactions are quite common and will be discussed below.

What is so unique about the 3c–2e bonding in $M–H_2$ and other σ-bond complexes that stabilizes them and sets them apart from species like carbocations and other main group analogs? It is *backdonation* (BD), i.e. the retrodative donation of electrons from a filled metal

d orbital to the σ* orbital of the H–H bond, similar to metal donation to π* orbitals in the Dewar–Chatt–Duncanson model for olefin coordination [3].

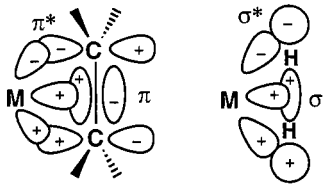

M–π bond M–σ bond

This is the crucial component in aiding the binding of H_2 to metals, in orienting the H_2 side-on to the metal, and in activating the H–H bond towards homolytic cleavage to dihydride ligands (oxidative addition). As shown by theoretical calculations, H_2 is an excellent π-acceptor, about as strong as ethylene or N_2. If the backbonding becomes too strong, e.g. if more electron-donating co-ligands are put on M, the σ bond cleaves to form a dihydride because of overpopulation of its antibonding orbital, σ*. Thus, a balance of σ donation and BD is needed to coordinate H–H and presumably other H–X or X–Y bonds to a metal. The entire reaction coordinate for the activation (elongation of the H–H bond) and oxidative addition of H_2 to a metal can be mapped out and related to the degree of BD. This single, basic bonding concept has guided our research and the work of over 100 other researchers worldwide in the field of σ-bond coordination both from theoretical and experimental standpoints. There are ~200 publications on theoretical analysis of M–H_2 coordination alone. Perhaps no other field of chemistry has had such effective interplay between experiment and theory as M–(η^2-H_2) and M–hydride systems. Obviously the innate simplicity of the H_2 molecule is the primary factor here, along with its importance in practical chemistry.

The activation and ultimate cleavage of the H–H bond is analogous to a high degree of olefin activation as represented by the metallocyclopropane extreme structure **3**, except that the C=C double bond in **2** can only be weakened to a near single bond and never is completely broken.

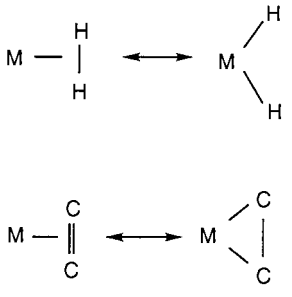

2 **3**

σ-Bond complexes can be viewed as 'arrested' OA, as originally suggested for Si–H bond coordination by Kaesz [5], but the arrest can be *anywhere* along the reaction coordinate. This is dramatically demonstrated by the remarkable 'stretching' of the H–H distance, d_{HH}, over a large series of complexes with H_2 bound to different metal–ligand fragments (Eq. (1)).

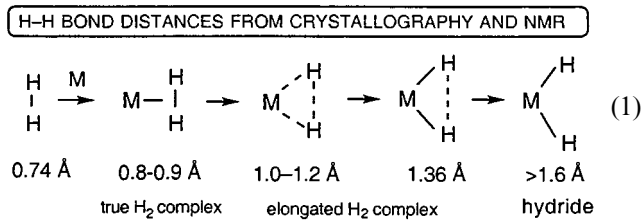

(1)

The d_{HH} is controlled primarily by the ability of the metal to backdonate electrons, particularly by the nature of the ligand *trans* to H_2 as will be shown in Section 2.6. Only d_{HH} in the range 0.85–0.90 Å (referred to as 'true' H_2 complexes or Kubas complexes, as exemplified by **1**) had been observed by diffraction methods and solid state NMR until around 1990 when *elongated H–H bonds* over 1 Å were found [1b]. $[Os(H_2)(en)_2(acetate)]^+$ (**4**) shows a very long d_{HH} and is on the verge of becoming a dihydride, which it was originally believed to be [4].

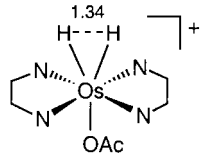

4

Complex **4** also created another paradigm shift because of the simplicity of its Werner-like ligand set: no bulky phosphines or exotic ancillary ligands are needed to stabilize nonclassical interactions. It must be kept in mind that 'elongated' is a relative term since the H–H bond is always stretched to some degree on coordination. Thus, not only can a chemical bond be snapped like rope, it can effectively be stretched like a rubber band until the bond is virtually gone, i.e. a dihydride forms. Remarkably, this can even be a dynamic equilibrium process:

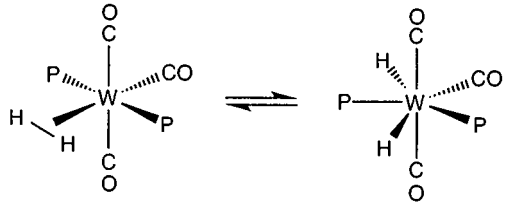

(2)

5 **6**

The tautomeric relationship between the H_2 complex **5** and the dihydride **6** is very significant because it proves that the activation and splitting of H_2 on M occur via side-on (η^2) bonding of H_2 to the metal [1]. Binding and cleavage of a σ bond on M can now be studied in exquisite detail, along with its microscopic reverse, σ-

bond formation and reductive elimination. It is astonishing to realize that one of the strongest chemical bonds is weakened and is breaking and reforming dozens of times a second without shining a laser on it or adding energy of any kind. As seen in Eq. (2), a large number of complexes displaying a near *continuum* of d_{HH} have now been structurally characterized throughout the entire transition metal series. We are thus able to 'see' breaking of a chemical bond by effectively taking snapshots along the entire reaction coordinate. The OA process can be arrested at various points along the reaction coordinate merely by varying the M–L sets and changing the electronics at M, which is a beautiful confirmation of the bonding model that is ultimately based on the Dewar–Chatt–Duncanson model. The factors that can stabilize H_2 and other σ complexes over OA are (1) electron-withdrawing ancillary ligands such as CO, particularly *trans* to the σ ligand; (2) positively charged metal centers, i.e. cationic rather than neutral complexes; (3) less electron-rich first or second row M; and (4) orbital hybridization, i.e. octahedral coordination and d^6 metals. Electrophilic fragments favor σ coordination, although highly electrophilic cationic centers generally give weak coordination and/or promote heterolytic cleavage of the X–H bond. Experimental evidence for the BD that controls OA has been well established by neutron scattering studies of the barrier to rotation of the H_2 ligand and will be discussed later.

1.3. Crucial role of backdonation in the coordination and activation of σ ligands

Whether H_2 binds molecularly to a particular metal fragment or oxidatively adds to give a dihydride can often be predicted by examining the NN, CO, or SO stretching frequencies of the corresponding N_2, CO, or SO_2 complexes as a gauge of a metal's backbonding ability. If there is one principle to keep in mind throughout reading this review and understanding σ-bond activation, it is *that BD controls σ-bond activation towards cleavage. A σ bond cannot be broken solely by sharing its two electrons with a vacant metal d-orbital.* Although the latter interaction generally is the predominant bonding component, a σ-bond complex is unlikely to be stable at room temperature without at least a small amount of BD. Thus, stable H_2 complexes of main group elements (e.g. pure Lewis acids such as BX_3) are unknown. Importantly, the linkage in $LM_n - H_2$ systems is identifiable as *the* bond between two species each capable of independent existence, $LM_n + H_2$. This principle should be remembered whenever a question arises concerning the validity of the 'true' σ complex, i.e. one not stabilized by a primary linkage such as in intramolecular σ bond interactions, commonly known as agostic interactions (Fig. 1), or an ionic bonding component. Coordination of σ bonds even in an agostic sense is also important from the standpoint of relieving electronic unsaturation in coordinatively unsaturated (16e or 14e) complexes. Complexes that might not otherwise be stable can be isolated, and indeed the 16e precursor to the first H_2 complex, $W(CO)_3(PCy_3)_2$ (**7**), is stabilized by an intramolecular agostic W···H–C interaction [6].

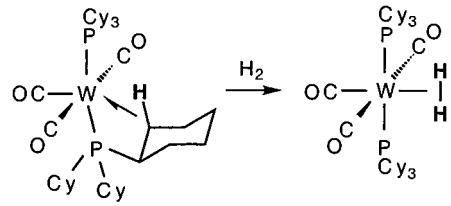

agostic complex (**7**) σ complex (**8**)

Intramolecular σ-bond interactions as in **7** were established to contain 3c–2e bonding by Cotton and coworkers in the early 1970s [7]. The term 'agostic' used for these interactions that was popularized by Brookhart and Green [8] should not however be used when describing external ligand binding *solely* through a σ bond as in **8**, which is best referred to as a 'σ complex.'

The number and variety of σ bonds already found to interact inter- or intramolecularly with metal centers is impressive [1b].

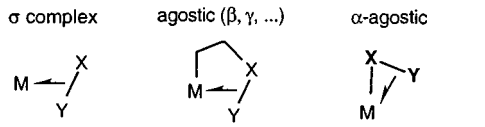

H–H, B–H	C–H, Si–H,	C–H, Si–H,
C–H, Si–H,	B–H, N–H	S–H, P–H,
Ge–H, Sn–H	C–C, Si–C	C–P, C–B, C–N

In principle, *any X–Y bond can coordinate to a metal center M* provided steric and electronic factors are favorable, e.g. substituents at X and Y do not block the metal's access. In all of these systems, BD plays a significant role in stabilizing the complexes, although for alkane complexes it is much weaker, primarily because of energy mismatch between the metal d and C–H σ* orbitals [9]. Thus, the H_2 molecule (as well as silanes and germanes) can be coordinated to M in stable fashion at ambient temperature, whereas a metal–alkane complex has yet to be isolated as a stable entity. There is the additional possibility that alkane ligands (particularly CH_4) may coordinate via more than one C–H bond, although computational studies do not show a significant preference for this. As will be shown, BD can involve p orbitals of the σ ligand, especially for metal coordination of B–H bonds in boranes. The coordination and activation of H_2 and other molecules containing simple two-electron σ-bonds on metal complexes is immensely important in

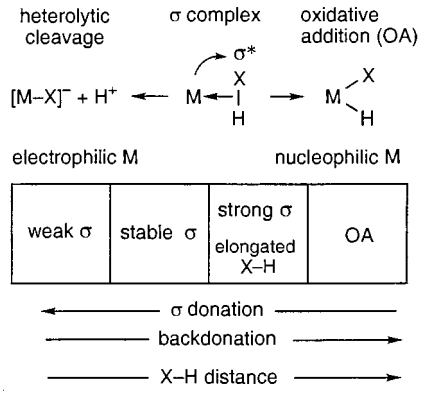

Scheme 1.

terms of fundamental science, especially catalysis. Hydrogen is considered to be the fuel of the future, and conversion of abundant but difficult to transport methane to liquid fuels is one of the most challenging areas in chemistry. The CH_3–H and H–H bond energies are practically identical (104 kcal mol^{-1}), and the C–H and H–H bonds are not too dissimilar in polarity.

An invaluable spectroscopic yardstick for measuring activation in M(η^2-X–H) bonds is *the value of the NMR coupling constant* J_{XH} compared to that in the free ligand. There is typically a 50–80% reduction in J_{HD} in unstretched HD complexes from the value of 43 Hz in HD gas, e.g. 34 Hz in $W(CO)_3(P^iPr_3)_2(HD)$ [1]. This reduction can often be directly correlated with d_{HH} as well as the closely-connected degree of BD. A 74% reduction occurs in $J(^{13}CH)$ for cyclopentane coordination in $CpRe(CO)_2(C_5H_{10})$, which is the first alkane complex to be observed by NMR spectroscopy (but decomposes above -80 °C) [10]. About a 65% reduction is found in $J(^{11}BH)$ for the coordinated B–H bonds in complexes of neutral borane σ ligands, such as $W(CO)_5(BH_3{\cdot}PMe_3)$ (see Section 5). However, as will be discussed in Section 4.2, J_{SiH} in silane complexes are always closer to those of the silyl–hydride OA products and more analogous to J_{HD} in elongated H–H bonds (ca. 10–20 Hz). Thus despite the obvious similarities, there are subtle differences in the properties and bonding in the various types of σ complexes.

1.4. Reactivity of σ-complexes: dependence on σ-donation versus backdonation

H_2 can bind in stable fashion to very electron-deficient M, which are weak backbonders nearly as well as to more electron-rich M. As will be discussed, calculations show that for highly electrophilic M, *the reduction in BD is almost completely offset by increased electron donation from H_2 to the electron-poor M*. Importantly, there are two completely different pathways for cleavage of H–H and X–H bonds: homolytic cleavage (OA) and heterolytic cleavage (Scheme 1).

Both pathways have been well identified in catalytic hydrogenation and may also be available for other σ bond activations such as C–H cleavage. Importantly, the pathway depends on the degree of BD: increased BD on nucleophilic metal centers favors OA and reduced BD on electrophilic centers favors heterolytic cleavage of η^2-bound X–H. Heterolytic cleavage of X–H bonds via direct proton transfer to a basic site on a *cis* ligand or to an external base is a crucial step in both industrial processes [11] and biological systems, especially in metalloenzymes such as hydrogenase with organometallic-like active sites [1b,12]. As a reflection of the dual activation pathways, H_2 is in essence the perfect ligand because it is *amphoteric*, i.e. essentially both a Lewis acid and a Lewis base. The great majority of coordinatively unsaturated transition metal fragments either molecularly binds or oxidatively adds H_2.

One of the most important questions is whether *direct transfer* of hydrogens from an η^2-H_2 ligand rather than the dihydride with a fully broken H–H bond takes place in catalytic hydrogenation as in Eq. (3).

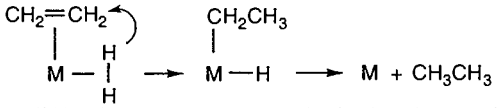

(3)

This is difficult to prove conclusively, but evidence exists that this can occur in some reactions, e.g. styrene hydrogenation [13] and hydrogenation of norbornadiene to nortricyclene [14]. Direct proton transfer from η^2-H_2 is known to occur in many systems because of the high acidity that can be exhibited by bound H_2, particularly on cationic complexes. In some cases, coordinated H_2 can become a stronger acid than sulfuric acid upon binding to cationic electrophilic metal centers, attaining a pK_a as low as -6, a decrease of over 40 units from the pK_a of free H_2 [15–17]! As shown in Eq. (4), the H_2 complex can then undergo heterolytic cleavage, for example protonate bases B such as ethers and form a monohydride or often a hydride-bridged complex [18].

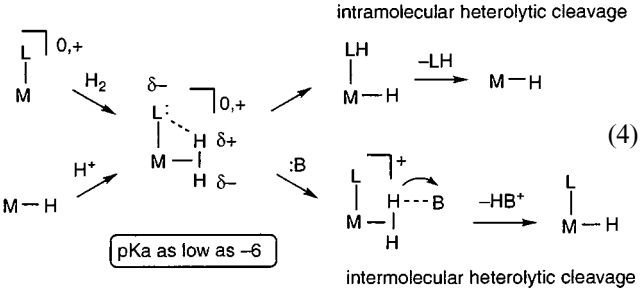

(4)

Intramolecular cleavage will occur if a *cis* ligand is more basic than an external base, e.g. if L has a lone pair to attract the partially positively-charged hydrogen. The kinetic acidity of an H_2 complex is greater than that of the corresponding dihydride. Eq. (4) shows

that a metal hydride can be protonated to form a cationic H_2 complex that is either stable (a common synthetic route) or may readily eliminate H_2. Here the kinetic site of protonation is normally the M–H bond, even though the thermodynamic site of proton transfer can be M (a H_2 complex forms initially and rearranges to a dihydride) [19].

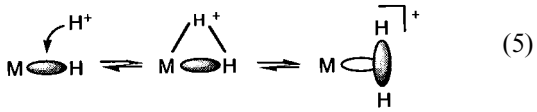

(5)

Other σ bonds can be cleaved heterolytically as in Eq. (4), particularly on electrophilic *cationic* M [1b]. For coordinated Si–H bonds, the coordinated bond becomes polarized in the opposite sense $Si(\delta^+)$–$H(\delta^-)$, i.e. the Si becomes positively charged.

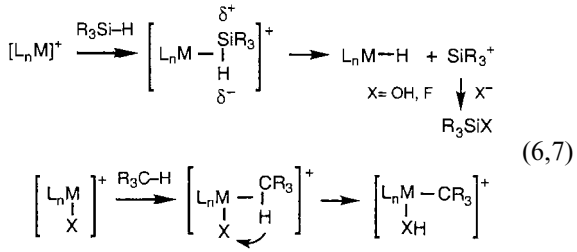

(6,7)

Very reactive silylium ions are effectively eliminated, which scavenge nucleophiles such as water or abstract fluoride from normally unreactive anions such as $B(C_6F_5)_4^-$ [18b]. Nucleophilic attack at coordinated Si may also occur in Eq. (6) and is probably more realistic. An important question is whether C–H bonds in alkanes, particularly CH_4, can be split in this manner and whether elimination of protons or carbocations will occur on 'superelectrophilic' metal centers. Intramolecular heterolytic cleavage of C–H in a fleeting σ alkane complex may occur in alkane conversions. In such systems *transfer of protons is very facile because of the extremely high mobility of* H^+, *and even short-lived, very weak σ complexes can be the crucial intermediates.* The C–H bond is thus more likely to be polarized towards $C^{\delta-}\cdots H^{\delta+}$ on electrophilic M, and H^+ immediately leaps to a basic *cis*-ligand X as soon as the alkane contacts M. Elimination of HX and subsequent functionalization of the metal-bound alkyl ligand can then be envisioned. An effective strategy for alkane activation is thus to design highly electrophilic complexes with accessible unsaturated sites that can bind an alkane via increased σ-donation and make the hydrogen on the C–H bond protonic and easily transferred off. Little is known about heterolytic C–H cleavage processes such as Eq. (7) because of the instability of alkane complexes, but low-temperature NMR studies of suitable systems may provide insight. Ancillary ligands that cannot give competing agostic C–H interactions such as tied-back phosphites may be important here [20]. Our current research interests are heading in this direction, inspired by the bonding model for σ-bond complexation that is in turn based on Dewar's π-bonding concepts.

2. Development of the bonding models for M–H_2 and σ-bond coordination and activation: the elegant interplay between theory and experiment

2.1. Theoretical studies of oxidative addition of H_2

The notion of coordinating molecules containing only 'inert' σ-bonds to M defied conventional bonding principles. Clearly a 'nonclassical' form of bonding, e.g. *3-center 2-electron bonding* had to join M to H_2 or other σ bonds, as for boron hydrides, carbocations, and H_3^+ (Fig. 1). Indeed, CH_5^+ is now considered to be an extremely dynamic H_2 complex of CH_3^+ [21], which bears an *isolobal* relationship with a transition metal center [2]:

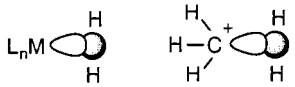

Despite foreshadowings, the high stability of M–H_2 bonding was initially astonishing. Several review articles focus at least partially on the theoretical aspects of H–H and C–H bond coordination and activation [22–26], including five in a special volume of *Chemical Reviews* devoted to computational transition metal chemistry [27]. The proof of existence of a M–H_2 complex is one of the few notable examples in science of the nearly simultaneous and independent derivation of theory and fact. Neither the theoreticians nor the experimentalists were aware of the seminal research being carried out during 1979–1983 when H_2 coordination and attendant activation were initially established. The classic theoretical paper by Saillard and Hoffmann in 1984 presenting extended Hückel calculations on the bonding of H_2 and CH_4 to metal fragments [9], was published only months after the seminal publication describing the W–H_2 complex [28]. This and several other mid-1980s papers (see below) gave valuable early insight into M–H_2 bonding modeled after M–ethylene coordination. Much like the experimental discovery, theoretical analysis of H_2 as a ligand developed over several years.

The initial bonding concepts for M–H_2 coordination remain widely accepted and extensive quantum chemical calculations have provided increasingly accurate quantitative descriptions beginning about 1987. The most recent calculations often show differences of only 0.01 Å between computed and experimental parameters such as d_{HH}. Many types of calculation methods have been employed to represent M–H_2 coordination, but density functional theory (DFT) has emerged as the leading methodology, allowing the treatment of increasingly complex systems with excellent success [29]. None-

theless, theoretical analysis remains challenging because the M–H_2 binding energy is small and much effort is required for proper modeling. In all cases, the electronic influence of the ancillary ligands such as phosphines is important, and the use of PH_3, the 'theoretician's phosphine,' to model PR_3 can give systematic errors, although useful information can still be obtained.

Qualitative ideas of catalytic H_2 activation on metals were devised in the late 1950s concerning the formation of transition states or intermediates prior to OA of H_2 to hydride complexes. Surprisingly, a molecular orbital analysis of this theoretical problem was not carried out until 1979 by Dedieu [30]. Both extended Hückel and ab initio Hartree–Fock calculations were carried out on H_2 addition to square-planar d^8 $RhCl(PH_3)_3$, a model for the well-known Wilkinson catalyst, where the phosphine is PPh_3. In this 16e complex, the H_2 approaches the filled d_{z^2} metal orbital. Calculations indicate that, at the beginning of the reaction, the end-on (η^1) approach of H–H is preferred over the side-on (η^2) approach (Eq. (8)).

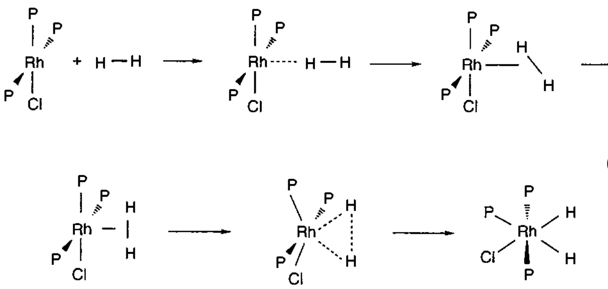

(8)

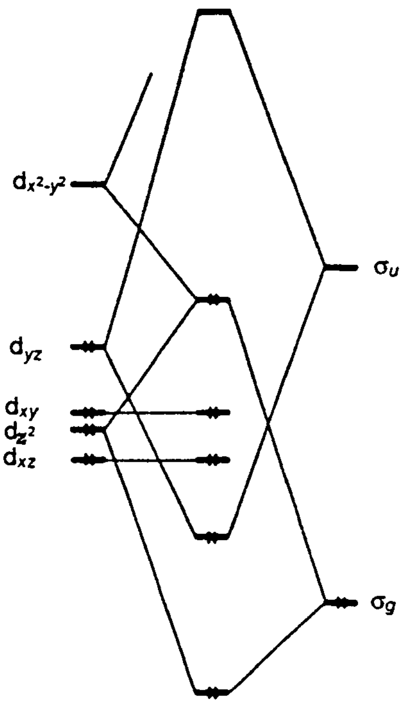

Fig. 2. Qualitative molecular orbital diagram for interaction of H_2 and $RhCl(PH_3)_3$.

In Eq. (8) the antibonding σ* orbital of H_2 and the antibonding combination d_{z^2}–σ(H_2) mix to give rise to a $d_{z^2}-\sigma^* + \sigma$ nonbonding level. When the distance between the reactants shortens, the geometry of the Rh–H_2 moiety gradually transforms from η^1 to η^2 via asymmetrically bound η^2-H_2. Crabtree also proposed such attack of H_2 on Ir [31].

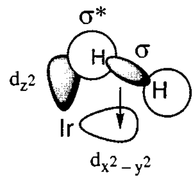

The H–H bond then symmetrically binds side-on and cleaves to give the *cis*-hydride isomer that SCF calculations had shown to be the most stable (Eq. (8)), which also was in agreement with experimental results. However, no true five-coordinate η^2-H_2 intermediate was found along the potential surface, i.e. H–H bond rupture to form a *cis*-dihydride was not arrested along the reaction coordinate. $RhCl(PPh_3)_3$ does not form a stable H_2 complex, so this result propagated the belief that H_2 coordination could only be transitory.

As shown in the MO diagram, the σ orbital of H_2 is destabilized and the σ* antibonding orbital is stabilized because d_{HH} has increased (Fig. 2). Importantly, the interaction of H_2 σ* with the filled d_{yz} orbital adds to the stabilization.

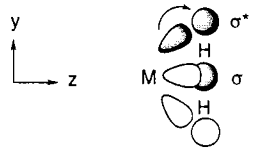

As has been emphasized, this *BD is critical to the binding and cleavage of H_2*. The lower the H_2 σ* level becomes, the more d_{HH} increases. Furthermore, distorting the $RhCl(PH_3)_3$ fragment as shown below reduces steric repulsion with the incoming H_2 and destabilizes and hybridizes the d_{yz} orbital in such a way that its overlap with σ* is increased:

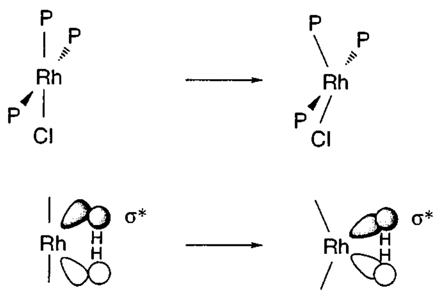

The overlap increases from 0.17 to 0.27 when the angle Cl–Rh–P decreases from 180 to 130°. Therefore, due to a larger overlap and better energy match, BD is enhanced, and even minor skeletal distortions can affect the degree of BD.

Subsequent investigations well support these early studies, and Hoffmann shows that the side-on approach of H_2 to both $Cr(CO)_5$ and $[Rh(CO)_4]^+$ fragments gives a deeper energy minimum than end-on [9]. Modern DFT computations of OA of H_2 on $[M(PH_3)_4]$ for M = Fe, Ru, Rh^+ show that the optimum reaction coordinate involves an η^1 approach early in the reaction, followed by H_2 swinging around to a η^2 conformation [32]. A steep drop in energy begins when d_{RuH} approaches 1.77 Å, whereupon the P–Ru–P angle decreases rapidly. However, d_{HH} does not change much until $d_{RuH} = 1.65$ Å, near its final value of 1.64 Å. Only then does elongation of d_{HH} take place, corresponding to a late transition state often found for σ-bond activation processes. The $Ru(PH_3)_4 + H_2$ reaction is highly exothermic (37 kcal mol^{-1}) and proceeds without an activation barrier because of the donor/acceptor characteristics of the metal species.

In contrast, the reaction profiles for OA of H_2 to *less electron-rich* cationic $[Rh(PH_3)_4]^+$ and $Ru(CO)_4$ fragments have small but distinct activation barriers (1–4 kcal mol^{-1}) and are less favorable thermodynamically (ca. 15 kcal mol^{-1} for Rh) [33]. A plateau corresponding to $Ru(H_2)(CO)_4$ with an elongated d_{HH} of 1.00 Å was found, attesting to the crucial influence of the ancillary ligands and charge on H_2 activation that will be discussed below. BD to such electrophilic fragments is reduced, which stabilizes the σ complex. Many other computations on the addition of σ ligands to unsaturated fragments demonstrate the existence of potential minima for σ complexes of H_2, CH_4, etc. prior to full OA. Both Hall and Dedieu give excellent overviews of OA and reductive elimination (RE) of H–H, C–H, and other σ bonds [27b,c].

2.2. $Pd(H_2)$, the first prediction of stable H_2 coordination

The first quantum-mechanical calculations showing that a M–H_2 interaction could be *stable* were described by Bagatur'yants [34,35]. He had hypothesized in 1980 a general bonding interaction of the two-electron type between low-lying localized orbitals of the σ-core of ligands such as C–H and unoccupied diffuse orbitals of the transition metal [34a]. Rough analysis indicated the interaction energy could reach 10–20 kcal mol^{-1}, which agrees well with subsequent experimental and calculated values for M–H_2 and related σ-ligand binding. Semiempirical CNDO quantum-mechanical studies of the coordination of H_2 to model complexes of Pd^0 and Pt^0 such as $M(PH_3)_n$ ($n = 1–3$) led to proposing a molecular H_2 complex to explain reversible binding of H_2 by certain Pd complexes [34b]. More reliable (but rudimentary by modern standards) non-empirical computations on H_2 interacting with a bare Pd atom showed a minimum for an η^2-H_2 structure on the potential curve at a Pd–H_2 distance of 2.05 Å, assuming an invariant d_{HH} of 0.74 Å (that in free H_2) [22,34].

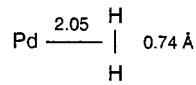

The critical finding was that *backdonation* (BD) from Pt $4d_{xz}$ to H_2 σ* is a very significant bonding component. As discussed by Dedieu, who has reviewed theoretical aspects of Pd and Pt chemistry [27c], the Pd–H_2 system was refined by several investigators [36–39], and almost identical results were obtained by Nakatsuji [36]. Despite discrepancies in the bond energies, the conclusion was that a Pd–H_2 complex should exist with d_{PdH} of 1.67–2.05 Å, H–Pd–H angles at 20–30° and d_{HH} up to 0.81 Å, which is only slightly less than in L_nM–H_2 complexes.

Direct experimental confirmation came from low-temperature matrix-isolated $Pd(H_2)$ complexes studied spectroscopically by Ozin [40] in 1986 and recently by Andrews [41]. Evidence for η^2-H_2 was obtained in a Xe matrix of Pd atoms, although Ozin suggested that η^1-H_2 may be present in Kr.

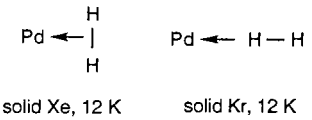

This remains the only experimental claim for η^1-H_2, which could be within 4 kcal mol^{-1} of being as stable as η^2-H_2 for $Pd(H_2)$. However, Andrews' studies in Ar matrices assign the IR bands found for '$Pd(\eta^1$-$H_2)$' to be due to higher $Pd(H_2)_{2,3}$ complexes. His DFT calculations on $Pd(\eta^2$-$H_2)$ show $d_{HH} = 0.85$ Å and $H_2 \rightarrow Pd$ σ donation versus BD of 0.17e and 0.23e, respectively.

2.3. Theoretical studies of $M(CO)_3(PR_3)_2(H_2)$ and bonding model for H_2 coordination

Not surprisingly, $W(CO)_3(PR_3)_2(H_2)$ was the first established H_2 complex studied theoretically, by a theoretician colleague at Los Alamos, Jeff Hay. Electronic structure models and ligand variation studies such as comparison of $W(CO)_3(PH_3)_2(H_2)$ with CO-free $W(PH_3)_5(H_2)$ led to important insights on H_2 binding and cleavage [42]. Hay's calculations utilized the Dewar–Chatt–Duncanson type of bonding model with bond lengths for the $W(CO)_3(PH_3)_2$ fragment based on diffraction data for $W(CO)_3(P^iPr_3)_2(H_2)$.

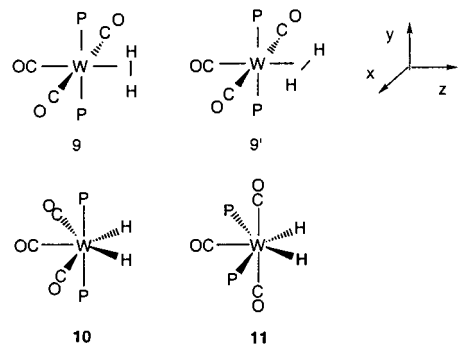

Table 1
Comparison between calculated and observed bond distances (Å) and dissociation energies (D_e, kcal mol^{-1}) for $M(CO)_nP_{5-n}(H_2)$ complexes (P = phosphine; $n = 0,1,3,5$)

Fragment	d_{MH}			d_{HH}			D_e		
	Calc [a]	Calc [b]	Expt [c]	Calc [a]	Calc [b]	Expt [d]	Calc [a]	Calc [b]	Expt
$Cr(CO)_5$	1.808			0.794			17.9		15 ± 1
$Mo(CO)_5$	2.006	1.899		0.787	0.824		15.7	19.6	
$W(CO)_5$	1.969			0.802			19.1		16
$Cr(CO)_3P_2$	1.782	1.857	1.75x	0.808	0.822	0.85	16.9	21.3	~17 [e]
$Mo(CO)_3P_2$	1.965	1.897		0.804	0.848	0.87	17.1	19.2	~17 [e]
$W(CO)_3P_2$	1.918	1.872	1.89n	0.832	0.862	0.89	21.3	20.9	~19 [e]
$Mo(CO)P_4$		1.896	1.92n		0.855	0.88			
CrP_5	1.730			0.829			18.7		
MoP_5	1.854			0.858			23.5		
WP_5	1.823			0.911			29.8		

[a] CCSD(T)/B3LYP level [43b].
[b] Relativistic NL-SCF + QR level [43c].
[c] X = X-ray, n = neutron.
[d] Solid-state ^{1}H-NMR, estimated deviation: 0.01 Å.
[e] Assuming a 10 kcal mol^{-1} correction for agostic interaction.

The η^2-H_2 geometry where the H_2 is parallel to the P–W–P axis (**9**) rather than perpendicular (**9′**) is most favored, and a bond energy of 16.8 kcal mol^{-1} is calculated. The dihydride forms (**10** and **11**) are less stable by 10–17 kcal mol^{-1}, although this was a large overestimation because the geometries **10** and **11** used at that time to represent the dihydride form have *cis*-hydrides, whereas they are now calculated to be distal as shown in **6** [43]. The computed value of d_{HH}, 0.80 Å, is close to the neutron diffraction value, 0.82 Å, although significantly lower than the presumably more accurate solid-state NMR value, 0.89 Å. Regarding the two possible H_2 orientations in **9** and **9′**, the latter is less stable by only 0.3 kcal mol^{-1}, although subsequent experimental and theoretical determinations of the barrier to rotation of H_2 indicate that this energy difference is about 2 kcal mol^{-1}. The preference for orientation **9** is consistent with the fact that the dπ orbitals in the $W(CO)_3(PR_3)_2$ fragments have the ordering $d_{xz} < d_{yz}$ if the PR_3 ligands are chosen to lie along the *y* axes. This ordering arises from the greater stabilization of d_{xz} afforded by the CO π* orbitals relative to the d_{yz} orbitals. In other words, there is less competition for BD with the strongly π-accepting *cis* CO ligands when the H_2 is aligned with the better donor ligands (phosphines), which is the observed geometry of most H_2 complexes. This is similar to *trans*-ethylene ligands coordinating 90° to each other in **12** to avoid competing for π-BD. The crystal structure of the $W–C_2H_4$ complex **13** shows that ethylene also coordinates along the P–W–P axis [44].

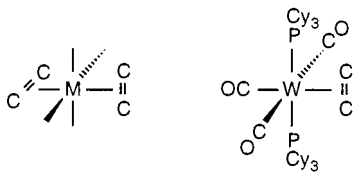

12 **13**

The electronic driving force, i.e. obtaining maximum W → ethylene BD, must be strong in **13** to counterbalance the steric demand of forcing the ethylene to align towards the very bulky tricyclohexylphosphines (cone angle 170°). The coordination sphere expands slightly to accommodate this orientation. W–P distances increase about 0.05 Å compared to that for the H_2 complex, and the $W–C_{ethylene}$ distances, 2.338(4) Å, are substantially longer than normally observed in W–ethylene complexes. In contrast to the 20% elongation (0.74 → 0.89 Å) of the H–H bond on binding to $W(CO)_3(PCy_3)_2(H_2)$ [1b], the C=C bond length, 1.378(6) Å, is only slightly stretched over that in free ethylene, 1.337(2) Å.

Replacing CO by PR_3, both experimentally and theoretically, leads to the seven-coordinate *dihydride* structure, $WH_2(PR_3)_5$, which is 3 kcal mol^{-1} more stable than the H_2 complex because of increased BD. If the d_{xz} orbital is to interact with the σ* H_2 orbital, the presence of the CO ligands serves to decrease this interaction as the d levels are stabilized by BD. Replacing the COs by PR_3 destabilizes the orbital and promotes BD, leading to H–H bond rupture, especially when the *trans* CO is replaced. Modern DFT and ab initio studies have since been applied to H_2 binding and activation on the models

$M(CO)_3(PH_3)_2$ (M = Cr, Mo, W) and $Mo(CO)_n(PH_3)_{5-n}$ ($n = 1, 3, 5$) [27c,43]. The calculated geometries and d_{MH} and d_{HH} are consistent with solid-state NMR data for the known $M(H_2)(CO)_3(PR_3)_2$ and $Mo(H_2)(CO)(dppe)_2$ complexes, with deviations of ~ 0.03 Å (Table 1). By comparison, the d_{HH} value originally calculated by Hay in $W(CO)_3(PH_3)_2(H_2)$, 0.81 Å, was too short. A valuable computational result is that the lowest energy structure for the dihydride tautomer in solution equilibrium with $W(CO)_3(PR_3)_2(H_2)$ has the trigonal bipyramidal (TBP) geometry **6** shown below (Eq. (2′)) [43a,b]:

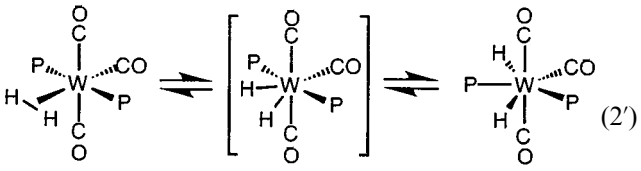

(2′)

1 **10** **6**

The first step presumably involves cleavage of H–H to give **10** followed by rearrangement to **6** by well-established mechanisms. The enthalpy difference between **1** and **6** is 1.29 kcal mol^{-1} in favor of **1**, in excellent agreement with experiment (1.2–1.5 kcal mol^{-1} for R = ^{i}Pr or Cy). The actual structure of $WH_2(CO)_3(PR_3)_2$ is unknown and originally was proposed to be a capped octahedron. The lower-energy TBP geometry in **6** is consistent with the NMR finding of inequivalent H ligands and PR_3 ligands and is similar to the structure of $MoH_2(CO)(depe)_2$ (**16**, below). Thus, the exact ligand arrangement is critical in the energetics of dihydrogen–dihydride systems and by analogy activation of all σ bonds.

2.4. H_2 is both a strong π-acceptor and a moderate donor ligand; relative strengths compared to other ligands

One question that arose from the above model of M–H_2 bonding was why are cationic H_2 complexes often as stable as their isoelectronic neutral analogs? This was demonstrated by Heinekey's studies of $[Re(CO)_3(PR_3)_2(H_2)]^+$ versus isoelectronic $W(CO)_3(PR_3)_2(H_2)$ where the more electrophilic cation binds H_2 as strongly as the neutral species wherein BD is greater [45]. The absolute and relative amounts of electron donation and BD are difficult to gauge quantitatively either theoretically or experimentally. One of the first experimental clues to the relative strength of BD was a comparison of ν_{CO} in $W(CO)_5(L)$ [46,47]. The L = H_2 complex prepared in liquid Xe had the highest ν_{CO}, on par with those for L = ethylene and N_2, and it was concluded that 'the $W(d_\pi) \rightarrow H_2$ (σ_u^*) interaction is stronger than expected theoretically' (alluding to the calculations by Hay [42a] and Hoffmann [2]) [46]. The similarity of H_2, N_2, and C_2H_4 coordination holds true in the $W(CO)_3(PR_3)_2(L)$ [48] and $Mo(CO)(dppe)_2(L)$ [49–51] systems, for which the axial (*trans* to L) ν_{CO} are compared to those in $W(CO)_5(L)$ [46,47,52,53] in Table 2. BD to L weakens BD from M to the *trans*-CO, which raises the ν_{CO}. In all cases, the complex with the strongest π-acceptor, SO_2, gives the highest ν_{CO}, while pure σ donors such as alkylamines give the lowest. Complexes with the somewhat weaker π-acceptors H_2, ethylene, and N_2 all have ν_{CO} within 10 cm^{-1} of each other. Importantly, the complexes with C–H bond interactions, either the matrix-isolated CH_4 complex [53] or the agostic complexes, have ν_{CO} characteristic of pure σ donor L ligands. In $W(CO)_5(L)$, ν_{CO} for L = CH_4 is even less than that for argon, which is close to being the ultimate weak pure σ-donor. Overall, the data suggest that *alkanes are poor backbonders* compared to H_2 and silanes, which oxidatively add to $W(CO)_3(PR_3)_2$. This matches Hoffmann's analysis showing that overlap between M d-orbitals and σ* of C–H is small but large for H–H [9], which helps explain why M–alkane binding is much weaker than M–H_2 binding.

More recent theoretical analyses show that H_2 is a much better π acceptor ligand than early calculations indicated. More quantitative measures of BD are provided by charge decomposition analysis (CDA) and extended transition state (ETS) analysis [54–60]. In Frenking's CDA studies, the canonical (natural) MOs of the complex are expressed in terms of the MOs of the appropriate fragments [55–57]. The MOs of the complexes, including Group 6 species with multiple H_2, $M(CO)_{6-x}(H_2)_x$ ($x = 1$–3), are formed by a linear combination of the MOs of $M(CO)_5$ and H_2 in the geometry of e.g. $M(CO)_5(H_2)$. The interaction is broken down into three components: charge donation (*d*), BD (*b*), and repulsive polarization (*r*). Table 3 shows each contribution at the MP2/II level for $M(CO)_5(H_2)$, *trans*-$M(CO)_4(H_2)_2$, and $W(CO)_5(L)$ for ligands with varying donor–acceptor properties. CDA indicates that CO is well balanced, both a good σ donor and a strong π acceptor, consistent with its ability to bind to most metal fragments (in this case electron-poor). Cyanide is

Table 2
Axial CO stretching frequencies (cm^{-1}) for complexes containing H_2 versus other ligands

L	$W(CO)_5(L)$	$W(CO)_3(PCy_3)_2(L)$	$Mo(CO)(dppe)_2(L)$
SO_2	2002	1873	1901
H_2	1971	1843	1815
C_2H_4	1973	1834	1813
N_2	1961	1835	1809
Argon/agostic [a]	1932	1797	1723
CH_4	1926		
Pyridine	1921	1757	1718
NR_3	1919 [b]	1788 [c]	1723 [b]

[a] L = argon (matrix) for $W(CO)_5(L)$; agostic C–H for others.
[b] $NR_3 = NEt_2H$.
[c] $NR_3 = NH_2Bu$.

Table 3
Charge decomposition analysis of $M(CO)_5(L)$ and *trans*-$M(CO)_4(H_2)_2$ complexes (electron units)

M	L	*d*	*b*	*r*
Cr	H_2	0.393	0.143	−0.147
Mo	H_2	0.315	0.105	−0.117
W	H_2	0.349	0.129	−0.105
W	CO	0.315	0.233	−0.278
W	N_2	0.027	0.107	−0.252
W	CN^-	0.488	0.024	−0.241
W	PH_3	0.278	0.091	−0.297
$Cr(CO)_4(H_2)_2$		0.277	0.209	−0.322
$Mo(CO)_4(H_2)_2$		0.362	0.149	−0.169
$W(CO)_4(H_2)_2$		0.483	0.191	−0.157

Table 4
Extended transition state analysis of donation versus BD energies (kcal mol^{-1}) for Group 6 dihydrogen complexes

Complex	E_D	$-E_{BD}$	Bond energy
$Mo(CO)_5(H_2)$	23.9	11.9	19.6
$Mo(CO)_3(PH_3)_2(H_2)$	17.6	18.9	19.2
$Mo(CO)(PH_3)_4(H_2)$	13.2	21.2	18.9
$Cr(CO)_3(PH_3)_2(H_2)$	16.9	17.9	21.3
Mo	17.6	18.9	19.2
W	18.2	19.5	20.9

a powerful donor but a weak acceptor, while N_2 is the opposite: a very poor donor and a moderate acceptor. Table 3 shows that H_2 is a slightly better acceptor than N_2 but unlike N_2, H_2 is a strong donor. This is beautifully corroborated experimentally by small molecular interactions with electrophilic $[Mn(CO)_3(PCy_3)_2]^+$, which binds H_2 weakly but not N_2, even at low temperature [61]. For $W(CO)_5(H_2)$, donation from H_2 (0.349e) is greater than BD (0.129e), as expected for this related electron-poor system. In the *trans*-bis-H_2 complexes, BD is increased and the M–H_2 bonds are stronger than in $M(CO)_5(H_2)$ [56]. Change in M is generally less significant, although Mo gives less BD. The negative sign of *r* indicates that charge is depleted from the overlap area of the occupied orbitals of the fragments. Depletion is large for CO and N_2, but much less for H_2.

In Ziegler's DFT-based ETS method, the M–H_2 bond energy can be decomposed into steric and orbital interaction terms plus a term for the energy required to relax the structures of the free fragments to the geometry of the combined molecule [54,59]. As for CDA, the orbital interaction can be further separated into donation (E_D), BD (E_{BD}), and other terms (all in kcal mol^{-1}) (Eq. (9)).

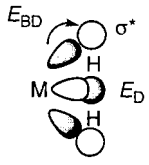

$$M-H_2 \text{ Bond Energy} = E_D + E_{BD} + E_{other} \quad (9)$$

Table 4 shows the relative dependencies of E_D versus E_{BD} on the ligand set is quite high, while the variation with M is relatively low. Overall the BD is much higher than earlier calculations suggested and can be *greater than σ donation*. Even for H_2 binding to the electron-poor $Mo(CO)_5$ fragment, E_{BD} is still one-third of the orbital energy. For the complex that models $Mo(CO)(H_2)(dppe)_2$, E_{BD} is nearly two-thirds of the orbital energy. Such substantial values for E_{BD} are supported by the observation of barriers to H_2 rotation as high as 11 kcal mol^{-1} in other systems (see below) which imply at least this much BD energy. An interesting comparison of the relative σ donation versus BD energies can be made with that for π donation versus π-BD recently *experimentally* measured for ethylene interaction with a Cu(110) surface [3c]. The results showed π donation from eyhtlene to Cu equivalent to 0.48 electron and $Cu \rightarrow \pi^*$ BD of 0.22 electron, i.e. BD is about one-third of the interaction. This ratio is similar to the ratio calculated for the σ bonding of H_2 to Mo in $Mo(CO)_5(H_2)$, indicating a relatively low degree of activation of the C=C bond in the Cu–ethylene surface interaction on a par with the low degree of activation of the H–H bond in the organometallic system. The energy of the Cu–C_2H_4 interaction was determined to be relatively low, 13 kcal mol^{-1}, which is about 5–6 kcal mol^{-1} less than the M–H_2 bonding energy in $Mo(CO)_5(H_2)$ [1b].

The sum of E_D plus E_{BD} remains nearly constant, varying from −34.4 to −36.5 kcal mol^{-1} for the Mo complexes. E_{other} takes into account steric factors, and is generally 13–17 kcal mol^{-1}, giving net M–H_2 energies of 19–21 kcal mol^{-1} close to the experimental value, e.g. 19.4 kcal mol^{-1} for $Mo(CO)_5(H_2)$. For very electrophilic centers, *loss in BD is almost completely offset by increased E_D from H_2 to the electron-poor center*. The M–H_2 energy for electron-poor $Mo(CO)_5(H_2)$ is surprisingly similar to that for the more electron-rich, isolable, phosphine complexes. From Table 2, SO_2 is a stronger acceptor similar to CO, but H_2 is not far back, closely followed by ethylene and N_2. As pointed out by Hoffmann [62], the reason CO is an excellent, ubiquitous ligand is the balance between its good donor/acceptor capabilities and its innate stability. H_2 offers the same advantages, on a lesser energy scale. Similar energy decomposition calculations for M–CO reveal increased σ-donation and decreased BD as electrophilicity of M increases, especially in cationic systems (nonclassical CO complexes) [62–64]. The computed first CO dissociation energy from $[M(CO)_6]^n$ (M = Group 4–9 metal; $n = -2$ to $+3$) is unexpectedly *higher* for the cations because donation from CO increases [64], as for the H_2 situation.

2.5. Dihydrogen versus dihydride coordination: an overview of the activation of H_2 towards oxidative addition

Once again experiment and theory went hand in hand during the mid-1980s in defining H_2 activation by examining the effects of fine-tuning the electronics at M. Computations showed that replacing acceptors such as CO by donors, i.e. increasing the basicity of M, promotes η^2-H_2 cleavage. This was dramatically demonstrated experimentally in $Mo(CO)(R_2PC_2H_4PR_2)_2(H_2)$ whereby merely changing R controlled whether a H_2 (**15**) or dihydride (**16**) complex was stable [51].

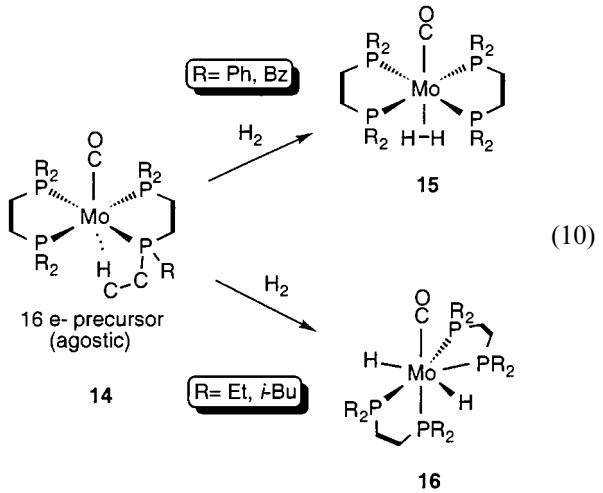

(10)

The more electron-donating alkyl diphosphines such as depe (R = Et) lead to increased BD, ultimately causing H–H rupture in **16**. Importantly, electronic rather than steric factors are crucial in stabilizing H_2 versus dihydride coordination since the phosphines with R = ^{t}Bu and phenyl (dppe) are similar in size. Changing M in $Mo(CO)(dppe)_2$ to W also leads to dihydride formation [65] because W is a better backbonder than Mo (third-row metals have more diffuse d orbitals). Numerous examples of fine-tuning of H_2 versus hydride coordination are known [1b] and provide excellent probes of electronics such as BD capability at specific fragments and stereo-electronic ligand effects. By variation of M/L, it is possible to *electronically 'arrest'* the reaction coordinate in Eq. (1) for OA of H_2 and examine it in fine detail, almost as if snapshots were taken along the pathway.

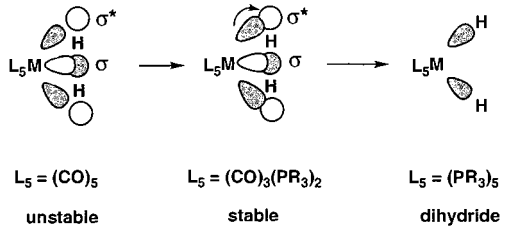

Virtually every gradation between these forms has been observed structurally and spectroscopically by varying M/L/charge. The stereochemistry of the ancillary L can influence whether a H_2 or dihydride complex is stable, but the degree of BD is clearly the dominant factor. N_2 is a π-acceptor like H_2, and parameters related to the electron richness of M such as ν_{NN} and electrochemical potentials can be used as indicators of π-basicity of the binding site in $M(N_2)L_n$ [15]. When ν_{NN} is less than 2060 cm^{-1} for the latter, a dihydride $M(H)_2$ (or elongated H_2 complex) will generally form on reaction of H_2 with ML_n, but when it is greater than 2060 cm^{-1} a true (unstretched) H_2 complex will be favored. The correlation is generally quite good for all M–L fragments, with occasional exceptions. An additional correlation was made that very electron poor fragments with $\nu_{NN} > 2160$ cm^{-1} could not bind H_2 in a stable fashion, but this is no longer the case. Electrophilic cationic complexes such as $[Mn(CO)(dppe)_2(H_2)]^+$ where the N_2 analog has ν_{NN} above 2160 cm^{-1} are stable (see Section 2.7).

2.6. The crucial influence of the ligand trans to H_2

The ligand *trans* to H_2 in $W(CO)_3(PR_3)_2(H_2)$ and $[FeH(H_2)(dppe)_2]^+$ [16] is either the strong acceptor CO or the high *trans*-effect hydride ligand. The d_{HH} are < 0.9 Å and their linearly related J_{HD} values are > 30 Hz, indicative of true H_2 complexes. A variety of H_2 complexes with different ligand sets show much longer d_{HH} and lower J_{HD}, 11–26 Hz. Although stretching of d_{HH} can generally be rationalized by increased BD, some structure-bonding aspects of H_2 coordination remain unaccountable. As shown above, $Mo(CO)(dppe)_2(H_2)$ is calculated to have high BD, yet it has one of the highest J_{HD} and shortest d_{HH} known. This lack of observable activation of the H–H towards OA and other observations can be explained in terms of the *trans effect*, i.e. the electronic influence of the ligand *trans* to the ligand of interest, which is crucial in coordination chemistry [66]. *The nature of the ligand trans to H_2 is the most important factor in determining where an H_2 complex lies along the reaction coordinate towards OA* [57,67–69]. For example, CO greatly reduces BD and has a powerful leveling effect that may even be underestimated in theoretical analyses. As seen from Table 5, *d_{HH} is normally < 0.9 Å and J_{HD} is > 30 Hz in complexes with CO trans to H_2, regardless of ligand set or overall charge*. Conversely, complexes with mild σ-donor ligands such as H_2O *trans* to H_2 or *π-donors* such as Cl, have elongated H–H bonds (0.96–1.34 Å) and J_{HD} from 9 to 28 Hz because of increased BD. A good comparison is between the Group 6 and 7 congeners, $Mo(CO)(H_2)(dppe)_2$ with $J_{HD} = 34$ Hz and $d_{HH} = 0.88$ Å and $TcCl(H_2)(dppe)_2$, where d_{HH} jumps to 1.08 Å from solution NMR evidence.

If the *trans* ligand is a strong σ-donor such as hydride, there is a powerful *trans* labilizing effect that reduces σ donation from H_2, which once again weakens

M–H_2 binding and contracts d_{HH}. Even relatively electron-rich neutral complexes with hydride *trans* to H_2 such as $OsHCl(H_2)(CO)(PR_3)_2$ and *trans*-$IrCl_2H(H_2)(PR_3)_2$ (**17**) often bind H_2 more weakly than comparable electrophilic cationic systems which rely on enhanced donation from H_2 for stability.

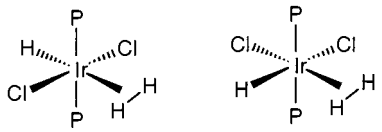

J(HD) = 34 J(HD) = 12

17 **18**

For the isomer with Cl *trans* to H_2, $IrCl_2H(H_2)(PR_3)_2$ (**18**), J_{HD} decreases dramatically to 12 Hz and ab initio calculations (R = H) show a spectacular increase in d_{HH} from 0.81 to 1.4 Å (1.11 Å from neutron data for R = ^{i}Pr) on going from **17** to **18** [67]. Clearly, the important concept is that the *influence of the trans ligand on H_2 activation is generally far greater than that of the cis-ligand set*, particularly in cations where BD is lower. This huge dependence on fragment stereochemistry can be expected to extend to other σ complexes, including alkane complexes where BD to C–H is much lower.

Table 5
H–D coupling constants and d_{HH} for H_2 complexes of selected octahedral rransition metal fragments

Metal fragment	J_{HD} (Hz)	d_{HH} (Å)	References
trans-CO ligands			
$M(CO)_3(PR_3)_2$ (M = Cr, Mo, W [a])	33.5–35	0.84–0.89 [b,c,d]	[117,167]
$Mo(CO)(PP)_2$	30–34	0.85–0.94 [b,c,d]	[50,168]
$[Mn(CO)(dppe)_2]^+$	32	0.89 [b]	[169]
$[Mn(CO)(depe)_2]^+$	33	0.87–0.89 [c]	[169]
$[Mn(CO)_3(PR_3)_2]^+$	33	0.87–0.89 [c]	[61]
$[Re(CO)_4(PR_3)]^+$	34	0.85–0.87 [c]	[18c]
$[Re(CO)_3(PR_3)_2]^+$	32–33	0.87–0.90 [c]	[45]
$[Re(CO)_2(PR_3)_3]^+$ [a]	31	0.90–0.92 [c]	[169]
$[Re(CO)(P\{(OR)_3\}_4]^+$ [a]	33	0.87–0.89 [c]	[170]
$[M(CO)(PP)_2]^{2+}$ (M = Fe, Ru, Os)	32–34	0.85-0.90 [c]	[70,171]
trans-Cl or other donor ligands			
$MCl(dppe)_2$ (M = Tc, Re)		1.08–1.21 [e]	[172]
$ReCl(PR_3)_4$		1.17 [d]	[173]
cis-$[Re(PR_3)_4(CO)]^+$	27.7	0.96–0.97 [c]	[174]
$[RuCl(PP)_2]^+$	16–26	0.99–1.17 [c]	[175,176]
$[OsCl(PP)_2]^+$	10–14	1.19–1.27 [c,d,e]	[80,171,176,177]
$[Ru(H_2O)_5]^{2+}$	31.2	0.90–0.92 [c]	[178]
$[Os(H_2O)(PP)_2]^{2+}$	14	1.19 [c]	[179]
$[Os(L)(NH_3)_4]^{+,2+}$	9–20	1.09–1.34 [c,d]	[180]
cis-$IrCl_2H(PR_3)_2$	12	1.11 [d]	[67]
$RuIH(PR_3)_2$		1.03 [d]	[83]
trans-Hydride			
$[MH(PP)_2]^+$ (M = Fe, Ru)	28–33.5	0.86–0.97 [c,d,e]	[15]
$[OsH(PP)_2]^+$	11–28	0.97–1.26 [c,d,e]	[15]
$MHCl(CO)(PR_3)_2$ (M = Ru, Os)	31–34.5	0.84–0.92 [c]	[181]
trans-$IrCl_2H(PR_3)_2$	34	0.85–0.87 [c]	[67]
$IrIH_2(PR_3)_2$		0.86 [d]	[124b]

[a] In equilibrium with dihydride tautomer in solution.
[b] Measured by solid-state NMR [117,167].
[c] Calculated from and bracketed by the empirical relationships, $d_{HH} = 1.42–0.0167J_{HD}$ [80] and $d_{HH} = 1.44–0.0168J_{HD}$ [182].
[d] X-ray or neutron diffraction.
[e] Calculated from T_1 data.

2.7. Other M/L/charge effects on H_2 binding and activation

When d_{HH} and J_{HD} couplings for Group 6–8 H_2 complexes with *trans*-CO ligands are compared (Table 5), a surprising consistency is observed. Because H_2 bonding is governed by both the Lewis acid strength of M for σ bonding (σ donation from H_2) and the BD ability of M (H_2 as an acceptor), the observed d_{HH} results from a balance of these components. The observation that isoelectronic but increasingly electron-poor neutral, cationic, and dicationic H_2 complexes (**12**–**14**) all possess comparable J_{HD} and d_{HH} raises an intriguing question.

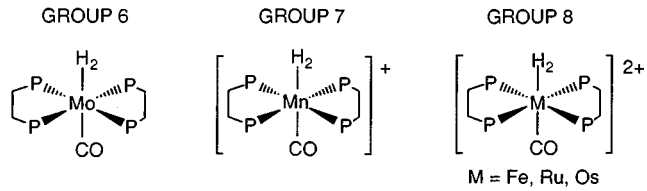

19 **20** **21**

Why do highly electrophilic Mn^+ and Fe^{2+} systems with poor BD ability have d_{HH} similar to neutral Mo and W systems with greater BD, the bonding component that is the main control of d_{HH}? One explanation is that the *activation of η^2-H_2 in the more electropositive systems is occurring primarily via increased σ donation from H_2 as compared to the more electron-rich systems*. As previously discussed, theoretical studies indicate that the σ-donation and BD components vary greatly depending on the electron-donating or withdrawing ability of the ligand sets, and the effect of M is much less. Importantly, the sum of the bonding energies of the two components remains nearly constant in a particular system, and for highly electrophilic M, *the loss in BD is compensated by increased σ donation from H_2 to the electron-poor M*. Thus the extremely electron-poor Fe *dication* (**21**) [70], which is stable in vacuo in contrast to the Mo^0 (**19**) and Mn^+ analogs (**20**) [69], actually binds H_2 more strongly than the neutral complexes that are stabilized by BD. Ab initio results for **19** versus **20** indicate that the M–H_2 binding energy for the Mn

cation is slightly higher than that for the neutral Mo analog (14.8 vs. 13.6 kcal mol^{-1}) [71].

The consistency in H–H activation on both the cationic and neutral fragments is astonishing, especially the narrow J_{HD} range of 32–34 Hz for most of the complexes listed in Table 5. The d_{HH} values for the cationic systems generally lie in a small range, 0.86–0.90 Å, nearer to the calculated d_{HH} of 0.87 Å in H_3^+ [72], which is an ideal model for H_2 activation strictly through σ-orbital interactions only.

Nonetheless, H_2 complexes of electrophilic fragments still contain some BD, e.g. as shown by the above calculated values in $Mo(CO)_5(H_2)$, which also indicates that the H_2 ligand competes well with CO ligands for BD. Such complexes are unstable mainly because dissociation of H_2 leads to highly reactive 'naked' $M(CO)_5$ fragments, but corresponding 16e fragments containing phosphines are stabilized by agostic C–H interactions. Thus, 'kinetic instability' rather than thermodynamic instability can be a problem for H_2 coordination to electron-poor metal centers.

The reaction coordinate for OA and the attendant d_{HH} (Eq. (1)) might appear to simply depend on the degree of $M \rightarrow H_2$ σ* BD, but this is deceptive. For example, why are d_{HH} not stretched past 0.9 Å in Group 6 complexes close to OA, such as $Mo(CO)(dppe)_2(H_2)$, for which the BD energy is calculated to be nearly twice that for σ donation? One answer is that such complexes with relatively short d_{HH} may actually lie further along the reaction coordinate than one might think. This is supported by normal coordinate analysis of $W(CO)_3(PCy_3)_2(H_2)$ which shows that the force constant for ν_{HH} is reduced by a factor of four from that in free H_2 and is similar to that for ν_{WH} [73]. The H–H and W–H_2 vibrational modes are highly coupled, and thus H–H bond breaking and W–H bond formation are intertwined and are well underway, although this is not reflected in d_{HH} and d_{MH} relative to other H_2 complexes. Rather than stretching like a rubber band, the H–H bond here *seems* to suddenly snap like a taut rope for the d^6 Group 6 metal systems, whereas it appears to be much more flexible for later transition metals. However, even in the Group 6 complexes the H–H bond can be stretched or shrunk with little energy cost and is probably delocalized. In solution, the activated W–H_2 system manifests a *tautomeric equilibrium* between a σ complex with a short H–H bond and the dihydride form (Eq. (2)). The reasons why some systems show this equilibrium and others exhibit bond elongation are unclear and will be discussed below.

The above principles when modified proportionately extend to silane or other σ complexes. Thus, 'stretched' Si–H bonds (2.10 Å) are known that roughly correspond to a d_{HH} of 1.05 Å in M–H_2. No matter how much analysis, the point at which to draw broken or unbroken lines representing partial versus full bonds for H_2 coordination in Eq. (1) and categorizations such as true σ complexes and stretched σ complexes will always be debatable, as it must be for continuum-like behavior. As will be shown below, elongated σ complexes present unique dynamical features that further emphasize the extraordinary complexity of σ complexes.

2.8. Elongated dihydrogen complexes: extraordinarily delocalized dynamic systems

Despite numerous sophisticated theoretical studies on H_2 complexes, there are few that properly model elongated H_2 complexes where the H–H bond length is often well over 1 Å [24,74–79]. The shape of the potential energy surface (PES) along the H–H coordinate in elongated H_2 complexes is crucial in understanding the structure and bonding in elongated complexes that exist in the 'gray zone' between dihydrogen and dihydride complexes. If these complexes are considered to be species where scission of H_2 is arrested at an intermediate stage between $M(\eta^2\text{-}H_2)$ and MH_2, the potential energy curve as a function of d_{HH} should have one minimum at the equilibrium distance. Perhaps the most accurate picture is based on the *rapid motion of two hydrogen atoms on a very flat PES with an exceptionally shallow minimum*. Hush, and later Lluch and Lledos show that the PES for the stretch of the H–H bond is exceptionally flat regardless of the method of calculation [77–79]. The possibility that elongated H_2 complexes could be described in such fashion was suggested by Morris and Koetzle in their NMR and neutron studies of *trans*-$[OsCl(H_2)(dppe)_2]^+$ [80], and subsequent computations suggest that the delocalization is even larger than had been imagined. The most definitive investigations are by Lluch and Lledos who combine DFT with quantum nuclear motion calculations of $[Cp^*Ru(H_2)(dppm)]^+$ and *trans*-$[OsCl(H_2)(dppe)_2]^+$ to obtain the nuclear vibrational energy levels [78]. These are rare cases of stretched H_2 complexes for which both a precise structure obtained by neutron studies ($d_{HH} = 1.10$ and 1.22 Å, respectively) and detailed temperature dependence of J_{HD} are available [80,81]. Furthermore, the Ru complex (though not the Os complex) exists in solution equilibrium with the *trans*-dihydride isomer in 2:1 ratio. The energies of dissociation of H_2 from $[Cp^*Ru(H_2)(dppm)]^+$ and $[OsCl(H_2)(dppe)_2]^+$ are 22.7 and 34.9 kcal mol^{-1}, respectively, denoting that the M–H_2 bond is relatively strong and the H–H bond is weak. However, there is unexpectedly poor agreement between the experimental and computed values of d_{HH} and d_{MH}. The computations indicate that the most stable structure is an unstretched H_2 complex ($d_{HH} = 0.888$ Å) for the Ru

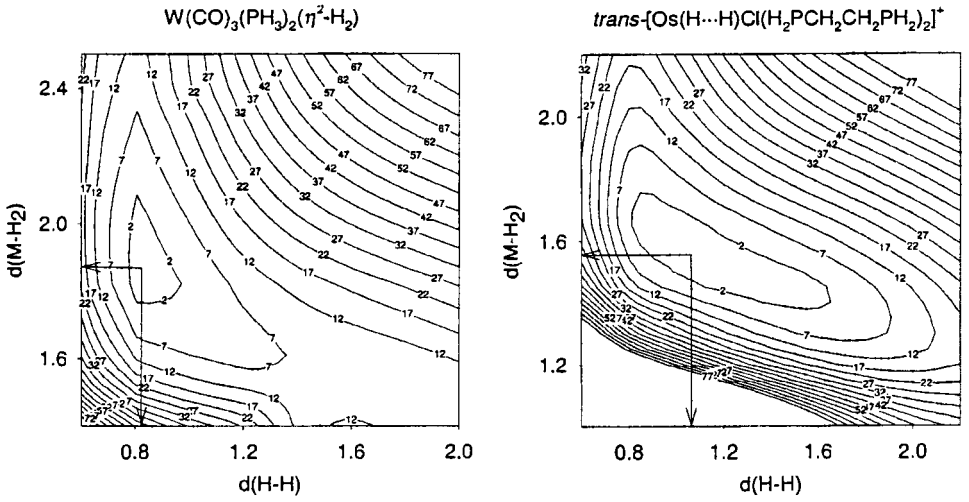

Fig. 3. Left: contour plot of the two-dimensional PES for $W(CO)_3(PH_3)_2(\eta^2\text{-}H_2)$. Energy contours appear every 5 kcal mol^{-1}. The arrows indicate the position of the minimum energy structure, where $d(HH) = 0.832$ Å, $d(W\text{–}H_2) = 1.872$ Å. Right: same for $[OsCl(H\cdots H)(H_2PCH_2CH_2PH_2)_2]^+$ ($d(HH) = 1.071$ Å, $d(W\text{–}H_2) = 1.567$ Å).

complex. For the Os complex, the energy minimum gives a d_{HH} of 1.071 Å, a distance characteristic of an elongated complex but much shorter than the neutron value for $[OsCl(H_2)(dppe)]^+$ of 1.22(3) Å.

Thus even high level calculations cannot explain what is seen experimentally. One of the consequences of the quantum nature of nuclei is that nuclei are not fixed and the overall structure of a molecule is vibrating even at 0 K. Therefore, nuclear motion calculations are important in understanding elongated $M\text{–}H_2$ systems. By solving the Schrödinger equation for the motion of nuclei on a reduced PES of two dimensions corresponding to the H–H and $Ru\text{–}H_2$ stretches, d_{HH} in the ground vibrational state is calculated to be 1.02 Å, much closer to the neutron value (1.10(2) Å). Importantly, the calculations show that the wave function here and for the Os complex are highly delocalized across a broad valley that lies oblique to the axes when compared to that for unstretched $W(CO)_3(PR_3)_2(H_2)$, which is fairly parallel to the $W\text{–}H_2$ axis with curvature along the H–H direction as d_{MH} shortens (Fig. 3). The crucial implication of these results is that the $\eta^2\text{-}H_2$ ligand is greatly delocalized and cannot be envisaged as a fixed, rigid unit in elongated complexes. The PES for the H–H stretch is so flat for the Os complex that the stretch of this bond can traverse *the entire distance range from 0.85 to 1.60 Å with attendant variation in d_{MH} at an energy cost of merely 1 kcal mol^{-1}*! The motion of the hydrogens is approximated in a cartoon-like fashion in **22**.

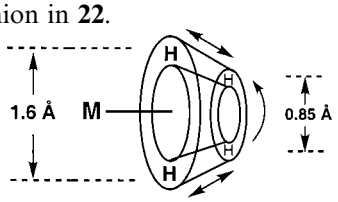

22

It is astonishing that a bond as strong as H–H can be weakened so as to be lengthened by 0.8 Å without a significant rise in energy. The $\nu(HH)$ and $\nu(MH_2)$ vibrational stretches in fact lose their meaning and the 'normal' stretching modes have to be redefined to one along the arrows shown in **22** (low-energy mode) and one orthogonal to it (high-energy mode).

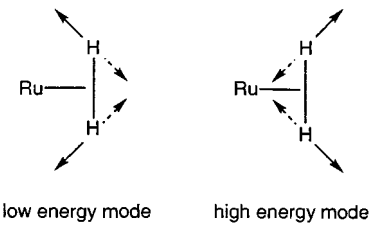

The soft vibrational mode parallels the reaction coordinate for OA. The hydrogens are also undergoing much slower librational/rotational motion with energy barriers of $\sim$4 kcal mol^{-1}, so the delocalization is occurring along an annular 'whirlpool' surface (neglecting $M\text{–}H_2$ deformational motion).

Thus, the initial picture that stretched complexes represent arrested states (with stationary structures) along the OA pathway should be revised to two hydrogen atoms moving almost freely in a large region within the coordination sphere of the metal. This behavior would logically be expected to be present in unstretched H_2 complexes, but to a lesser degree. The existence of solution equilibria between distinct dihydrogen–dihydride tautomers even for complexes with relatively short d_{HH} such as $W(CO)_3(PR_3)_2(H_2)$ can be understood as a manifestation of this delocalization, although a double minimum potential well is present here. The question remains why such equilibria occurs for some systems (e.g. $[Cp^*Ru(H_2)(dppm)]^+$) and not

others ($[OsCl(H_2)(dppe)_2]^+$). One answer is that forces other than the electronics at M must be considered, e.g. steric factors, structural rearrangement barriers for six versus seven coordination, or overall bond energetics. Sizable rearrangements of the coordination sphere takes place for the $Mo(CO)(PP)_2$ system on OA of H_2 (Eq. (10)). The two hydride ligands are *distal* to each other in the pentagonal plane of **16** and *cis* to the CO but in **15** the hydrogens are proximal and *trans* to CO. These rearrangement energies and other forces cannot easily be quantified or identified to be present in many cases.

2.9. Interaction of a coordinated σ bond with a cis ligand: the cis-effect in dihydrogen–hydride complexes

From both experimental and theoretical calculations, complexes that contain a hydride *cis* to a H_2 ligand often show structural distortions and orientations of η^2-H_2 indicative of an interaction [67,82–91]. The barrier to H_2 rotation can be perturbed by the presence of a hydride *cis* to H_2, as will be discussed later. From crystallography, the H_2 is eclipsed with the P–M–P axes in (**A**) and (**B**) in Scheme 2 but staggered with respect to the *cis* ligands in (**C**) where the rotational barrier is unusually low.

EHT calculations by Eisenstein show this unusual staggering and low barrier to result from the '*cis*-effect,' a two-electron interaction between σ_{Fe-H} and σ^* H_2 [170,171].

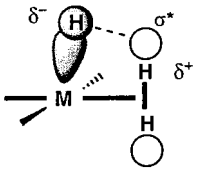

cis-interaction

This stabilizes the conformation where H–H eclipses Fe–H and creates a nascent bond between the closest nonbonded H centers. In the absence of a *cis* hydride, $M \rightarrow H_2$ BD controls the H–H conformation which optimally is eclipsed with the P–M–P axis (phosphines are good electron donors into the d-orbitals that backbond). In (**C**), BD would ordinarily position H_2 to lie in the P2–Fe–P3 plane, but the *cis* effect favors eclipsing of H–H and Fe–H bonds (the orthogonal direction). The observed crystal structure reflects a balancing of the effects, and the H_2 lies in an intermediate position [84].

The spherical nature of the hydride s orbital favors bond overlap with nearby vacant orbitals without severely stretching or breaking M–H, which is also advantageous in σ-bond metathesis reactions discussed below. Ab initio calculations by Eisenstein give a better understanding of this effect by examining the orientations and barrier to rotation of H_2 in (**B**) versus (**C**) in Scheme 2 [27a,85]. In (**B**), the orientation of H_2 should be controlled electronically principally by BD only (no steric effects here). Calculations confirm this, giving a twofold barrier of 1.9 kcal mol^{-1} close to the experimental value, 2.4 kcal mol^{-1}. The optimal structure is the conformation with the H–H axis parallel to P–Fe–P. For (**C**) the best conformation at the *SCF level* is where the H_2 is closely aligned with the *cis* Fe–H bond and the top of the barrier height (1.6 kcal mol^{-1}) occurs when H_2 almost aligns with P2–Fe–P3. However, at the *MCSCF level*, the preferred H–H orientation is rotated clockwise 64° away from alignment with P1–Fe–H_c, which agrees well with the crystal structure (Scheme 2), and the top of the barrier (1.4 kcal mol^{-1}) is 90° beyond this. These two different types of calculations illustrate the two competing interactions present in (**C**): the $Fe \rightarrow H_2$ BD that prefers the H_2 to be perpendicular to Fe–H and an electrostatic interaction (the *cis*-effect) favoring coplanarity of H_2 and Fe–H. The latter effect, which manifests as a dipole–induced-dipole interaction, receives more emphasis in the SCF calculations. For MCSCF, the agreement with experiment is good because no ligand *cis* to H_2 is tilted towards it, so that all d orbitals are properly set for efficient BD.

The 16e H_2 complex $RuHI(H_2)(PCy_3)_2$ shows crystallographically that Ru–H is bent toward the H_2 ($\angle$ I–Ru–H1 = 99°) [86].

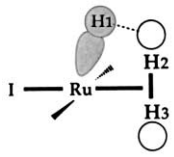

23

The nonbonding H1···H2 distance in **23** is short (1.66(6) Å) because of *cis*-interaction while H2···H3 is elongated (1.03 Å). Extended Hückel calculations demonstrate that this structure is the minimum.

2.10. Intramolecular hydrogen exchange, polyhydrogen complexes, and σ-bond metathesis

The above *cis*-effect is significant because of its apparent role as the nascent interaction in intramolecular hydrogen exchange processes (Scheme 3).

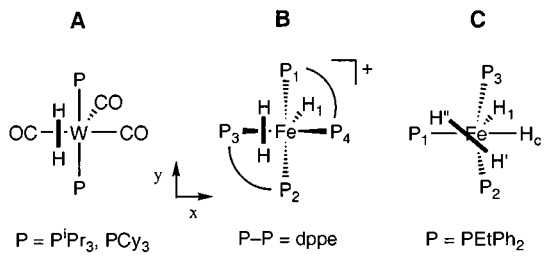

Scheme 2.

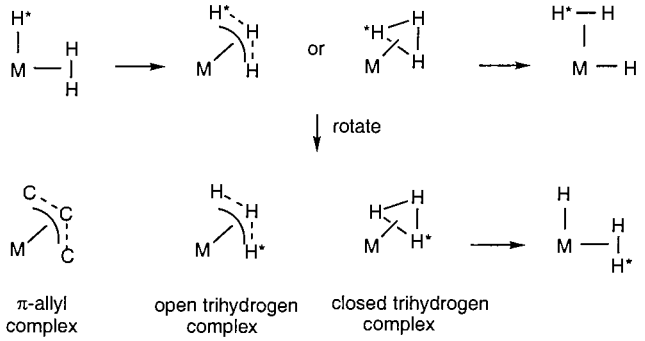

Scheme 3.

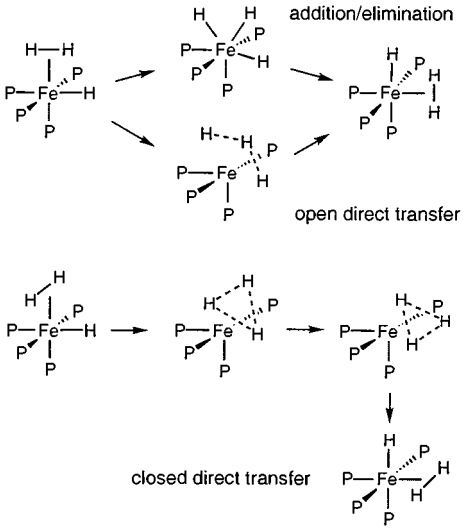

Scheme 4.

The intermediate is essentially a trihydrogen complex, which was initially proposed by Brintzinger as the key species in this direct hydrogen transfer process [92]. The possible existence of η^3-H_3 ligands has been examined theoretically by Burdett in his detailed studies of polyhydrogen species, H_n ($n = 3$–13) [93,94]. A trihydrogen complex is yet to be isolated, although there is experimental evidence for its intermediacy in a facile tautomerization reaction [95].

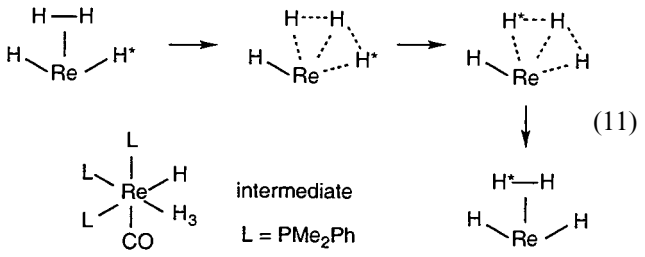

(11)

The $ReH(H_3)$ species is estimated to be no more than 10 kcal mol^{-1} less stable than the $ReH_2(H_2)$ complex. Unlike triangulo H_3^+, a trihydrogen ligand is more likely to have an open linear structure best represented as H_3^- as supported by calculations. The M–H_3 moiety with its kite-shaped 'trefoil' topology can then effect transfer of hydrogen to the *cis* position to give η^2-H_2 where hydride was originally present. Facile exchange of hydrogen atoms H* with H, hence isotopic scrambling, can take place either by this route or by rotation of the H_3 followed by reformation of the original hydride–H_2 orientation. The *H_3^- ligand is analogous to the π-allyl ligand* in charge distribution and bonding properties. Simplistically, H_3^- represents a bond, no-bond delocalized structure just as allyl represents single-bond, double-bond delocalization (Scheme 3). There is thus a remarkable parallel between σ-bond coordination and that of π-bond coordination with all its facets that extend well beyond simple complex formation.

OA to a trihydride would also produce exchange, but this is a much higher energy path in ab initio calculations on $[FeH(H_2)(PH_3)_4]^+$ [96]. The trihydride is 65.3 kcal mol^{-1} higher in energy than that of the reactants, which alone makes the existence of such an intermediate unlikely. By comparison, the open direct transfer pathway for H-exchange has an activation barrier of *only 3.2 kcal mol^{-1}* (the triangulo 'closed' intermediate is much higher at 69 kcal mol^{-1}) (Scheme 4).

DFT calculations on $[FeH(H_2)(PMe_3)_4]^+$ with the actual PMe_3 ligands instead of PH_3 models show an even lower barrier, ~ 0.5 kcal mol^{-1} [96], which corresponds well with the observation of extremely fast H/H_2 scrambling even at -140 °C [97].

Also, within thermodynamic limits, H* in Scheme 4 could be any other metal-bound atom (Z) such as halide or a group such as alkyl and H–H could be any other σ ligand (X–Y) such as alkane. This represents *σ-bond metathesis* [98–102], *a more general form of the above hydrogen exchange analogous to olefin metathesis.*

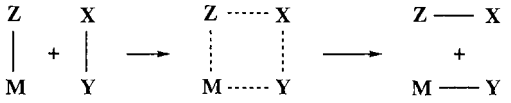

(12)

Mechanistically, two different kinds of σ-bond metathesis are possible. While the four-center intermediate in Eq. (12) looks to be similar to the trefoil intermediate in the hydride–H_2 exchange, the actual bonding and the overall pathway may differ depending on the electronics of the system. A 'traditional' mechanism of σ-bond metathesis is that shown above, which is similar to that postulated for heterolytic cleavage of H_2 ($X = Y = H$) where σ-complex intermediates were not involved (before H_2 complexes were discovered). This pathway works mainly with early transition metals, lanthanides, and actinides with little BD ability, e.g. complexes of the type Cp_2MR. In the case of metathesis of $Cp_2LnH + H_2$, the calculated transition state is best viewed as a nearly linear H_3^- ligand with short d_{HH} and strong M–H interaction through the wingtip H centers [102k]. The other potential mechanism is similar to the hydride–H_2 exchange (Eq. (11))

which does involve σ-complex intermediates, and this could occur on more electron-rich M such as $[FeH(H_2)(PH_3)_4]^+$.

3. Experimental evidence for backdonation

Except in rare cases, the η^2-H_2 ligand rapidly rotates (librational motion is more accurate) even in the solid state, further delocalizing the H atom positions. In elongated H_2 complexes, the highly delocalized, rotating H_2 ligand can occupy a large volume of the coordination sphere as discussed in Section 2.8. One of the key diagnostics for coordination of H_2 is in fact the observation by inelastic neutron scattering (INS) of rotational transitions for η^2-H_2 [103–108], which cannot exist for classical hydrides. Most importantly, these extensive studies by Eckert and coworkers measure the barrier to rotation of H_2 ligands and consequently offer *direct experimental proof of* $M \rightarrow H_2$ *BD*. The rotational transitions and barrier are very sensitive to even minor changes in ligand environment about M and provide valuable insight into the reaction coordinate for splitting of H_2 on M and intramolecular interactions. A good example is the initial experimental evidence for interaction between η^2-H_2 and *cis* hydride ligand provided by INS, which will be discussed below.

3.1. H_2 rotation in $M(\eta^2$-$H_2)$

The H_2 ligand undergoes rapid two-dimensional hindered rotation about the M–H_2 axis, i.e. it spins (librates) in propeller-like fashion with little or no wobbling. Most significantly, there is a small barrier to rotation, ΔE, brought about by $M \rightarrow H_2$ σ* backdonation (BD).

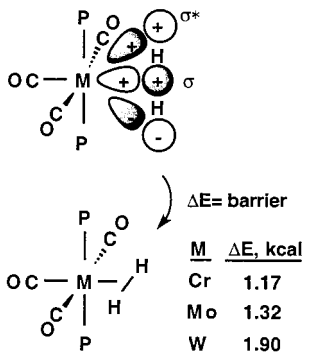

The σ-donation from H_2 to M cannot give rise to a rotational barrier since it is completely isotropic about the M–H_2 bond. The barrier actually arises from the *disparity* in the BD energies from the d orbitals when H_2 is aligned parallel to P–M–P versus parallel to OC–M–CO, where BD is less (though not zero). ΔE varies with M and other factors and can be analyzed in terms of the BD and other forces that lead to it, both by theoretical calculations or by a series of experiments where M/L sets are varied. In most 'true' H_2 complexes with $d_{HH} < 1.0$ Å, the barrier is less than 3 kcal mol^{-1} and observable only by neutron scattering methods. It can be a low as 0.5 kcal mol^{-1} for symmetrical ligand sets, e.g. all *cis* L are the same, but has never been measured to be zero because minor geometrical distortions are usually present. In the case of complexes with elongated H–H bonds [109] or where rotation is blocked as in $[Cp'_2M(H_2)(L)]^+$ (M = Nb, Ta) (see below), much higher barriers up to 11 kcal mol^{-1} are observed. Interactions of η^2-H_2 with *cis* L can significantly lower the barriers on the other hand. INS is normally limited to measurement of barriers < 3 kcal mol^{-1}.

This hindered rotation of η^2-H_2 is governed by various forces, which can be divided into bonded (electronic) and nonbonded interactions ('steric' effects). The direct electronic interaction between M and H_2 results from overlap of the appropriate molecular orbitals. Nonbonded interactions such as van der Waals forces between the η^2-H_2 atoms and the other atoms on the molecule may vary as η^2-H_2 rotates. *Inter*molecular interactions should not contribute much to the barrier to rotation of η^2-H_2 because the H_2 ligand is close to the metal and fairly well insulated from outside contact. However, intermolecular contacts may have a minor effect on the coordination geometry about M, which could in turn, slightly affect the electronics of M–H_2 bonding.

3.2. Determination of the barrier to rotation of dihydrogen by inelastic neutron scattering

The geometry and height of the barrier can be derived by fitting the rotational transitions observed by INS to a model for the barrier [105,106]. The simplest possible model for the rotations of a dumbbell molecule is one of planar reorientation about an axis perpendicular to the midpoint of the H–H bond in a potential of twofold symmetry (Fig. 4). In this figure, the H_2 performs large-amplitude librations within its potential minimum that are constrained to a plane perpendicular to the three-center M–H_2 bond. Strong support for this hypothesis is provided by solid-state NMR from which the out-of-plane librational amplitude can be estimated to be less than 6° [110]. In all other cases [111–113] where rotations of H_2 have been observed, both rotational degrees of freedom exist since the H_2 is not chemically bound. The energy level diagram for the twofold potential with one rotational degree of freedom is shown in Fig. 5. The energy levels are given by BJ^2 for zero barrier height (B = rotational constant). The transition between the lowest two levels, i.e. $J = 0$ and $J = 1$, is akin to the *ortho–para* H_2 transition for (nearly) free hydrogen. Its rotation has two degrees of

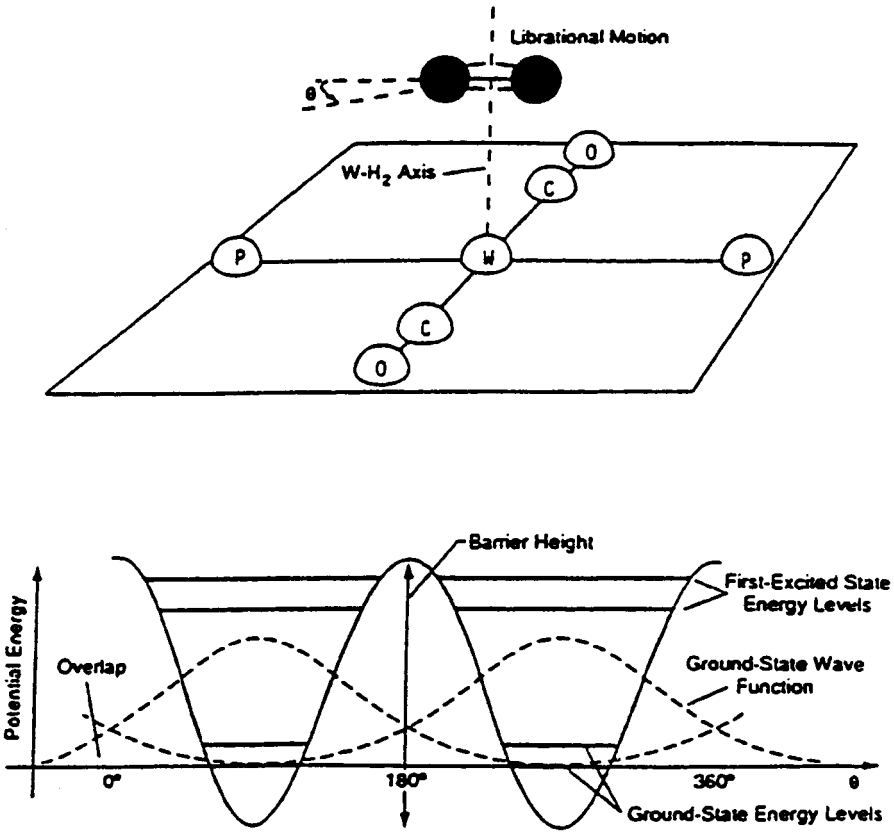

Fig. 4. Model for the hindered rotation of the H_2 ligand in metal complexes. Schematic of H_2 rotation in $W(CO)_3(\eta^2\text{-}H_2)P_2$ about the axis from the W atom to the midpoint of the H–H bond in (top); double-minimum rotational potential with energy levels (not to scale) and wavefunctions (bottom).

freedom and the energy levels therefore are given by $BJ(J+1)$. The *ortho*→*para* H_2 transition cannot be observed directly by optical methods, as it involves a change in the total nuclear spin of H_2, which is forbidden in optical spectroscopy [111].

Application of a barrier to rotation rapidly decreases the separation between the lowest two rotational levels, which may then be viewed as a split librational ground state. Transitions within this ground state (Fig. 4, bottom) as well as those to the excited librational state (often called torsions) may be observed by INS. The former occur by way of rotational tunneling [114] since the wave functions for the H_2 in the two wells 180° apart overlap. This rotational tunneling transition has an approximately exponential dependence on the barrier height, and is therefore extremely sensitive to the latter. It is this property that is exploited to gain information on the origin of this barrier.

Both the rotational tunneling transition and the transitions to the first excited librational state can readily be observed by INS techniques [103,104,108,114]. Neutrons are extremely well suited as probes for molecular rotations when the motion involves mainly H atoms. These modes (torsions, librations) normally do not involve large changes in the polarizability or dipole moment of the molecule, and are therefore often difficult to observe by optical techniques. The INS studies allow observation of low-lying transitions

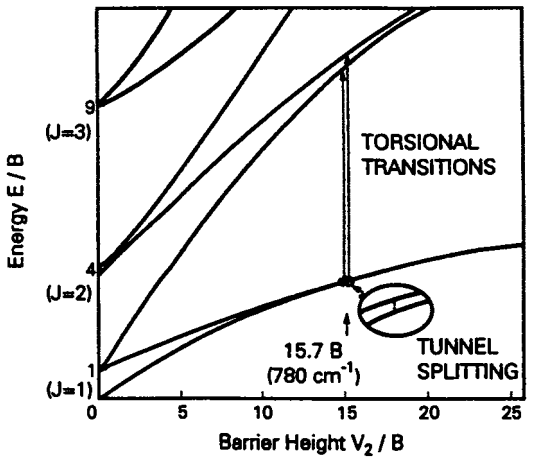

Fig. 5. Energy level diagram for rotation with one degree of freedom, φ, of a dumbbell molecule in a double-minimum potential $V_2(\varphi)$. The transitions indicated are for $W(CO)_3(H_2)(PCy_3)_2$, where B is taken to be 49.5 cm^{-1}.

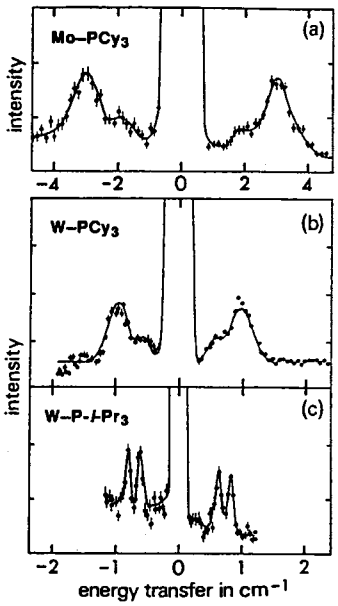

Fig. 6. Rotational tunnelling spectra for the series of complexes $M(H_2)(CO)_3(PR_3)_2$ where M = Mo and R = Cy (top) and M = W and R = Cy (middle) or ^{i}Pr (bottom). Note the change in energy scale between top and middle figures.

within the ground librational state of the η^2-H_2 (tunnel splitting), which corresponds to the *para* ($I = 0$, $J = 0$) to *ortho* ($I = 1$, $J = 1$) transition for free H_2 (120 cm^{-1} in liquid hydrogen). INS measurements are typically carried out at ~ 5 K using ~ 1 g of polycrystalline H_2 complex sealed under inert atmosphere in aluminum or quartz sample holders. Low-frequency INS measurements are performed on the cold neutron time-of-flight spectrometers at the Institute Laue Langevin in Grenoble, France, and the Laboratoire Leon Brillouin. All the high-frequency data (> 200 cm^{-1}) discussed below were obtained in the Filter Difference Spectrometer at the Los Alamos Neutron Scattering Center. This measurement is only possible by use of a differential technique [115] involving subtraction of the spectra observed for a sample with a D_2-ligand (or another suitable 'blank') from that of an identical sample with the H_2 ligand, which leaves only the vibrational modes for M–(H_2).

In most cases the ground-state rotational tunnel splitting, as well as the two transitions to the split excited librational state, are observed. Because the tunnel splittings (typically 1–10 cm^{-1}) can be measured with much better accuracy than the librational transitions, the value for the barrier height V_2 is usually extracted from the former. For M(η^2-H_2) complexes, ground librational state splittings between 17 and 0.6 cm^{-1} are observed at temperatures as high as 200 K. The signals shift to lower energy and broaden but remain visible into the quasielastic scattering region. Observation of rotational tunneling, which is a *quantum-mechanical* phenomenon, at such a high temperature is extraordinary: in all previous studies of this type involving for example rotations in CH_3 or $[NH_4]^+$ groups, the transition to classical behavior occurs well below 100 K. The barriers to rotation of coordinated H_2 derived from the tunnel splittings observable by INS range from 0.6 to 2.4 kcal mol^{-1}.

3.3. Origin of the barrier to rotation of η^2-H_2

3.3.1. Metal–H_2 binding

As mentioned previously, the rotational barrier for H_2 is nearly completely intramolecular in origin: primarily the direct electronic interactions between H_2 and M, and to a lesser extent, the nonbonded interactions between the H atoms and the neighboring atoms on the same complex. The INS rotational tunneling spectra of several variants of $M(H_2)(CO)_3(PR_3)_2$ (M = Group 6; R = Cy, ^{i}Pr) demonstrate the pronounced effect of the change in M (Fig. 6), as strongly supported by the theoretical calculations described below. The ratios of the tunnel splittings is ca. 1:3:5 for W–Mo–Cr, whereas variation of the phosphine shifts the mean tunneling transition by about 20%. As previously discussed, the rotational barrier is mainly sensitive to BD and is affected by σ-bonding only to the extent that it weakens and lengthens the H–H bond, thereby changing the value of *B*. However, the barrier to rotation is only a relative measure of the BD interaction because it results from the difference in energy between H_2 oriented in its minimum versus its maximum energy configurations, as discussed in more detail below.

Electronic calculations support the above conclusion because calculated barrier heights, which do not include nonbonded interactions, show good agreement with experiment, as summarized in the review by Maseras et al. [27a]. Ab initio and Fenske Hall calculations performed on $M(H_2)(CO)_3(PR_3)_2$ (M = W, Mo and R = H, Me, ^{i}Pr and Cy) [42b,104] confirm the experimentally observed equilibrium orientation of η^2-H_2 along the P–M–P axis, as well as give values for the barrier heights in remarkable agreement with those derived from INS data. For example, the barriers from the Fenske–Hall calculation [42c] are 1.0 and 1.5 kcal mol^{-1}, respectively, for M = Mo, W and R = Cy compared with the experimental values of 1.5 and 2.2 kcal mol^{-1} (later revised to 1.3 and 1.9 kcal mol^{-1} as discussed below). The energy barrier is a direct manifestation of the energy difference in the BD for H_2 aligned along the P–M–P axis versus the OC–M–CO axis, where BD is poorer because of competition from the strong π-acceptor CO ligands.

Virtually all the electronic calculations of barrier heights compare remarkably well with those derived from INS, which strongly supports the notion that the barrier arises from a variation in the overlap between

$\sigma^*(H_2)$ and the relevant metal d orbitals upon rotation of η^2-H_2. The d orbital energies in turn are affected by at least three different factors: the nature of M orbital structure, the effects of coligands on M (and thus on M–H_2 binding), and, to a much lower extent, perturbations on the coordination geometry around M by counterions or solvent molecules via crystal-packing forces.

3.3.2. Effect of the M

Systematic studies of the effect of M d-orbitals on H_2 binding and the barrier to rotation have been carried out on Group 6 and 8 complexes. Results for H_2 complexes with the same ligands but different M were compared with the aim of establishing trends in M–H_2 bonding in general, and more specifically, the BD interaction to which the barrier is most sensitive. For $M(H_2)(CO)_3(PCy_3)_2$, the values for a simple twofold barrier increases down the group from 1.17 kcal mol^{-1} for the Cr-analog to 1.32 for Mo and 1.9 kcal mol^{-1} for W [42c,116,117]. The BD may therefore be said to increase in the order Cr < Mo < W. From this, one might be tempted to conclude that H–H bond activation would increase in the same order (recall that the H–H bond of $W(CO)_3(PCy_3)_2(H_2)$ cleaves in solution to give equilibrium amounts of the dihydride tautomer, while the Cr and Mo congeners do not). This might be indicated, for example, by decreasing values of ν_{HH} in the order Cr < Mo < W. However, IR studies [118–120] of $M(CO)_5(H_2)$, show that ν_{HH} decreases in the order Mo > Cr > W (Table 6). Similarly, one might suppose that the strength of the M–H interaction would increase with an increasing amount of BD. Vibrational data (Table 6) for $\nu_s(MH_2)$ in the PCy_3 complexes, however, show that this mode has approximately the same value for the Cr and W complexes, and is significantly lower for the Mo analog. Table 6 also shows that the enthalpies of H_2 binding for the series $M(CO)_3(PCy_3)_2(H_2)$ do not track well with $\nu(MH_2)$ or the rotational barriers, where Mo is out of order.

These results in conjunction with solution stabilities (W > Mo > Cr) suggest a complicated picture of H_2 binding in terms of trends in physical properties versus electronic interaction down Group 6. A major problem for correlating properties of the H_2 complexes is separating $H_2 \rightarrow M$ σ-bonding effects from those of BD. The σ interaction is the major contributor to the total M–H_2 bond interaction, and $H_2 \rightarrow M$ σ-bonding strength does appear to correlate as Cr ~ W > Mo in accord with the observed values of $\nu(MH_2)$ and $\Delta H_{binding}$ for $M(CO)_3(PCy_3)_2(H_2)$. Calculations also indicate that Cr fragments are slightly better σ-acceptors than W [121], but the opposite is true for the backdonating ability of M, which correlates with the observed larger barrier height in the W complex. The stronger σ interaction in the Cr complex on the other hand would contribute to the total M–H_2 bond strength but would not affect the barrier to rotation because $H_2 \rightarrow M$ σ-bonding is isotropic about the M–H_2. The effect of BD on $\nu(MH_2)$ is unclear. One would have anticipated $\nu(MH_2)$ to be significantly higher for $W(CO)_3(PCy_3)_2(H_2)$ than for the weaker backbonder, $Cr(CO)_3(PCy_3)_2(H_2)$, as found for $Cr(CO)_3(PCy_3)_2(H_2)$ in comparison to $Cr(CO)_5(H_2)$.

Some of these apparently conflicting observations can be explained by the same issues concerning vibrational spectroscopy of the M–H_2 moiety. Mainly, the importance of ν_{HH} as a good indicator of H–H bond activation and $\nu(MH_2)$ as a measure of M–H_2 binding energy is doubtful, because the H–H stretching coordinate involves a large amount of W–H stretching as well. Thus, the frequencies are highly mixed, e.g. the difference in ν_{HH} between $W(CO)_5(H_2)$ and $W(CO)_3(PCy_3)_2(H_2)$ would have been expected to be much greater than 21 cm^{-1} because of far superior BD to H_2 in the more electron-rich phosphine complex. This is in marked contrast to end-on bound ligand stretches such as ν_{NN} or ν_{CO} that correlate well with the electron richness of M. N–N stretching involves little or no displacement of M and should therefore be a good measure of N–N bond activation.

Summarizing, it appears that in the series $M(CO)_3(PR_3)(H_2)$ the M–H_2 σ-interaction is weaker for Mo

Table 6
IR frequencies, rotational barriers, and enthalpies of binding of Group 6 H_2 complexes

Complex	ν(HH) [a]	$\nu_{as}(MH_2)$ [a]	$\nu s(MH_2)$ [a]	Barrier [b]	$\Delta H_{binding}$ [c]
$Cr(CO)_5(H_2)$	3030	1380	869, 878		
$Cr(CO)_3(PCy_3)_2(H_2)$		1540	950	1.17(10)	-7.3 ± 0.1
$Mo(CO)_5(H_2)$	3080				
$Mo(CO)_3(PCy_3)_2(H_2)$	~2950 [d]	~1420 [d]	885	1.32(10)	-6.5 ± 0.2
$Mo(CO)(dppe)_2(H_2)$	2650		875	0.7(1)	
$W(CO)_5(H_2)$	2711		919		
$W(CO)_3(PCy_3)_2(H_2)$	2690	1568	951	1.9(1)	-9.4 ± 0.9

[a] In cm^{-1}. In Nujol mulls for phosphine complexes and liquid Xe [119] or rare gas matrices [120] for the pentacarbonyls.
[b] In kcal mol^{-1}.
[c] Enthalpy of H_2 binding, kcal mol^{-1} [183].
[d] Estimated from observed D_2 isotopomer bands.

than Cr or W, while BD is slightly better for Mo and much better for W than Cr based on rotational barriers. The very high lability of H_2 in the Cr analog could be ascribed to this weaker BD, supporting the general notion that BD is more crucial than the M–H_2 σ-interaction in influencing relative stabilities of complexes, d_{HH}, and possibly overall bond strengths (e.g. W–H_2 > Cr–H_2).

The barrier to H_2 rotation on Group 8 metals has been determined for only the Fe and Ru complexes $[MH(H_2)(PP_3)]^+$ (**24**) (M = Fe, Ru; $PP_3 = P[CH_2CH_2PPh_2]_3$), $[FeH(H_2)(dppe)_2]^+$ (**25**) (dppe = $Ph_2PCH_2CH_2PPh_2$) and $FeH_2(H_2)(PEtPh_2)_3$ (**26**) [84,103, 104,122].

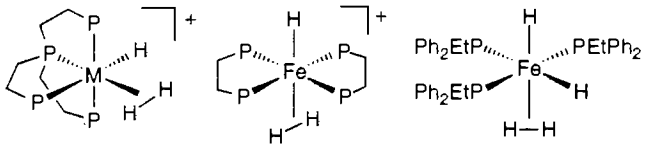

24 25 26

Surprisingly for **1** the barrier is higher in the Fe than the Ru complex which suggests that *first row Fe is a better backdonor to H_2 than second row Ru*, unlike for Group 6 complexes [122]. The ν_{NN} of the N_2 analogs, i.e. 2110 and 2182 cm^{-1}, respectively, for the Fe and Ru complexes imply that more N–N bond activation is again present in the Fe compound on account of better BD, but in this case into the π* orbital of N_2.

The barrier for **26** is only 1.1 kcal mol^{-1}, an important finding in regard to the *cis*-interaction between the H_2 and hydride ligand here. In **26** the H–H bond is staggered with respect to the *cis* Fe–P and Fe–H axes in opposition to both electronic and steric considerations. The influence of the d orbitals that favors eclipsing of the H–H bond with the P–Fe–P bond thus competes with the attractive *cis*-interaction. Consequently, the electronic potential shows a broad minimum and the maximum is necessarily lower, as reflected by the rotational barrier which is lower than it would be due to either competing factor alone (in comparison to H_2 complexes without *cis* hydride attractions).

Rotational barriers are often lower than expected based on BD arguments for reasons other than the above. Theoretical considerations [50,87] show that the electronic barrier to H_2 rotation should be essentially zero if the ligands in the plane parallel to that of the rotation are highly symmetric, regardless of strength of BD to H_2. Complexes of the type *trans*-$ML(H_2)(dppe)_2$ thus have low barriers (< 1 kcal mol^{-1} for M = Mo; L = CO). However, the barrier for $Tp^*RhH_2(H_2)$ (**27**) is only 0.56(2) kcal mol^{-1} despite its unlikely symmetry about the M–H_2 axis and its apparently weak H–H bond as judged by $\nu_{HH} = 2238$ cm^{-1} and d_{HH} of 0.94 Å calculated from the value of the rotational constant, 37.1 cm^{-1}, from INS data [123].

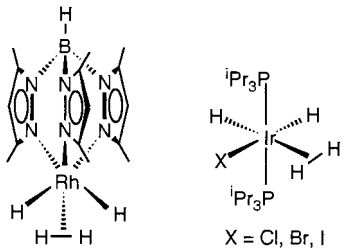

27 28

The most plausible explanation is that interaction of H_2 with the *cis*-hydrides lowers the barrier. Another well-studied system is $IrXH_2(H_2)(P\text{-}^iPr_3)_2$ (**28**) where the barrier for X = Cl is 0.51(2) kcal mol^{-1}, the lowest measured [124,125].

3.3.3. Ligand effects

The calculations described above deal with the direct electronic interaction between η^2-H_2 and M and therefore reflect the effect of the ancillary ligands L (especially L *trans* to H_2) on the electronic state of M as well (see Sections 2.3, 2.4, 2.5, 2.6 and 2.7). Careful analysis of these ligand effects in relation to measured barriers to H_2 rotation provides detailed information on the origin and strength of the critical $d_\pi(M)$–$\sigma^*(H_2)$ interaction. Measurements of the barriers for H_2 complexes with the same M but different L should relate the observed differences to the electronic effects of these L. An excellent case of such ligand effects studied theoretically is $TpRhH_2(H_2)$ versus $CpRhH_2(H_2)$, where the barrier for the experimentally unknown complex with the more electron-donating Cp ligand is calculated to be 4.88 versus only 0.45 kcal mol^{-1} for the Tp derivative [126]. The computed value is remarkably close to the experimental value of 0.56 kcal mol^{-1} for the Tp* complex (**27**) which contains methyl groups on the pyrazole rings. DFT calculations on $TpRhH_2(H_2)$ give a rotational tunnel splitting of 9.2 versus 6.7(5) cm^{-1} found experimentally [123], demonstrating their accuracy for obtaining dynamic and spectroscopic parameters for polyhydride complexes.

Morris has applied the concept of ligand additivity effects to derive generalizations of the stability of octahedral d^6 H_2 complexes [127]. Electrochemical parameters E_L for each type of L are added and a value for the electrochemical potential $E_{1/2}(d^5/d^6)$ is calculated by empirical formulae derived by Lever [128]. This quantity gives an overall measure of the electron-donating ability of the ligand set, and ranges of $E_{1/2}$ for stable H_2 binding may be defined. In order to assess the possible relevance of this overall measure of electron-donating ability of a M–L fragment to measurements of the barrier to rotation, data for three Fe, two Mo and two Ru complexes with different sets of ligands are given in Table 7. The measured barriers are listed along with the

Table 7
Comparison of the barrier to rotation with electrochemical parameters and ν(NN)

	Barrier [a] (kcal mol^{-1})	Σ^5 E_L [b]	ν(NN) [c] (cm^{-1})	$E_{1/2}$ (N_2–complex)
Fe				
$[FeH(H_2)(dppe)]_2^+$	1.8	1.04	2120	1.5
$[FeH(H_2)(PP_3)]^+$	2.1	0.8	2110	1.2
$FeH_2(H_2)(PEtPh_2)_3$	1.1	0.28	2058	0.6
Mo				
$Mo(CO)(H_2)(dppe)_2$	0.6–0.8	2.43	2120	0.1
$Mo(CO)_3(H_2)PCy_3)_2$	1.5–1.7	3.55	2159	0.9
Ru				
$RuCp(CO)(H_2)(PCy)$	(>3.5)	1.37		2.0
$[RuH(H_2)(PP_3)]^+$	1.4	0.8	2182	1.4
$RuH_2(H_2)_2(PCy_3)_2$	1.1	0.58		1.2

[a] Barrier heights for the Fe complexes were renormalized to the same value of rotational constant B (49.5 cm^{-1}) as determined from neutron diffraction measurements.
[b] Sum is over all the coligands of H_2.
[c] For the analogous N_2–complex.

sum of the E_L for the five ligands other than H_2, the computed $E_{1/2}$ for the N_2 complex, and the experimental value for ν_{NN} if available. All of these are taken from papers by Morris [15,127]. Inspection of Table 7 reveals no obvious correlation between either the overall electron-donating ability of the M fragment as derived from the ligand additivity method or the values of ν_{NN} and the measured barrier to rotation. There are several likely reasons for this, perhaps the most important of which is that the apparent strong correlation between the electron-donating ability of the M fragment and ν_{NN} is at best a measure of BD into the π^* orbital of N_2. Since that orbital is lower in energy and has a much greater spatial extent than $\sigma^*(H_2)$ an analogous degree of BD in the H_2 analog is not assured. Thus, even though ν_{NN} gives an indication of the *stability* of its M–H_2 counterpart, it evidently cannot be used to draw conclusions about BD to $\sigma^*(H_2)$.

Correlating the complexes in Table 7 is difficult because of the fact that there are substantial geometric differences in the ligands sets, for example between the Ru complexes, Another critical geometric effect relates to the fact that the barrier to rotation measures essentially a difference in BD for η^2-H_2 between its orientation at the maximum and minimum of the rotational potential function. If BD is strong, but does not differ much in these two orientations as in **29**, the rotational barrier may be quite low (0.6–0.8 kcal mol^{-1} in **29**), provided the ligand set is symmetrical and not very distorted.

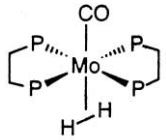

29

If the changes made to the ligands are not as drastic as going from the symmetrical $FeH(dppe)_2$ fragment to the $FeH(PP_3)$ fragment, then the barrier should be a good relative measure of the degree of BD, as it is for comparisons of the effect of changing the M keeping the ligands the same [122]. The $IrXH_2(H_2)(P^iPr_3)_2$ system (**28**) where only X is varied does show small changes in barrier [124,125]. DFT calculations on $IrXH_2(H_2)(PMe_3)_2$ models reproduce the barriers from INS data quite well [125].

	X		
	Cl	Br	I
Experimental barrier (kcal mol^{-1})	0.51(3)	0.48(3)	1.0(4)
Calculated barrier (kcal mol^{-1})	0.37	0.42	0.66
H–H (Å)	0.78	0.82	0.86

The barriers for the PH_3 model are much higher (>2 kcal mol^{-1}), demonstrating a high sensitivity to the nature of the phosphine which requires the use of a realistic phosphine such as PMe_3 in calculational estimates for the barrier. The increase in barrier for X = I may be evidence for increased BD. The d_{HH} as determined by theoretical calculations (Cl) or by neutron diffraction (Br, I) increases by about 0.04 Å for each halide change, which might indicate increased BD down the series. However, the possible coupling of rotational dynamics with highly dynamic site exchange between H_2 and hydride ligands may blur the correlation with INS data.

The complexes $[Cp'_2M(H_2)(L)]^+$ (M = Nb, Ta) show *blocked rotation of the H_2 ligand* in the NMR spectrum, and the free energy of activation of the H_2 internal rotation is determined to be 8–12 kcal mol^{-1} both experimentally and by theoretical calculations [129–131]. At 178 K, decoalescence of signal is observed for the HD complex but not for the HH species. The high rotational barrier can be attributed to the complete loss of BD on going from the global minimum to the transition state in which the H_2 is bound only by σ donation from H_2 (Calc. $d_{HH} = 0.79$ Å) [131].

4. Si–H bonding to metals in σ-silane complexes compared to M–H_2 bonding

4.1. Silane coordination to metal complexes

Like H_2, silanes do not have nonbonding electron pairs or π-electrons to ligate to metal centers, but hydrosilanes (which include SiH_4 and organosilanes with at least one Si–H bond) can bind to M to form stable σ complexes through Si–H bonds to give 3c–2e M(η^2-Si–H) bonding. The bonding and activation of hydrosilanes has been well reviewed in journals [132–136] and is extensively covered in Kubas's book [1b]. The Si–H bond is activated towards cleavage remarkably similarly to the H–H bond, and tautomeric equilibria can exist with the OA product for the silane complex in Eq. (13), which is the first transition-metal SiH_4 complex and a model for methane coordination [137].

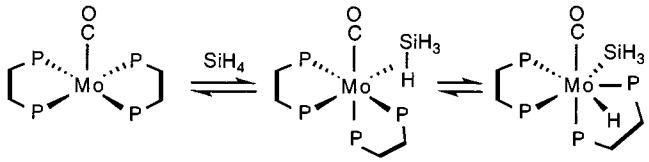

(13)

The Si–H bond elongates on coordination to the same relative extent as the H–H bond does, and the energetics of binding, cleavage, and exchange with *cis*-hydrides are also quite similar. This would not have been expected on the basis of the large difference in steric and electronic factors. Simultaneous coordination of both H–H and Si–H bonds is known [138], and the coordination and activation of Ge–H and Sn–H bonds in germanes [139–142] and stannanes [143–148] are also directly analogous to Si–H.

A major difference in comparison to M–H_2 complexes is that M–H–Si and M–H–X linkages are asymmetric, i.e. look like hydride-bridged systems with M–H–Si near 90° (Eq. (14)).

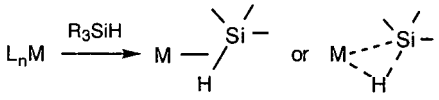

(14)

Also the presence of substituents R on Si gives rise to large variations in the bonding electronics and also can give steric influences. The value of d_{HH} in $W(H_2)(CO)_3(PR_3)_2$ is ca. 20% longer than that in free H_2, similar to the lengthening of d_{SiH} in the neutron structure [149] of $(CpMe)Mn(CO)_2(SiHFPh_2)$ (1.802(5) Å cf. 1.48 ± 0.02 Å in free silanes). However, typical J_{SiH} for the Mn–silane complexes, 40–70 Hz, are far lower than those for free silanes, ~200 Hz, whereas J_{HD} for M(η^2-HD) (30–35 Hz for true H_2 complexes) is much closer to the value for free HD (43 Hz) and correlates linearly with d_{HD}. Thus, the situation for silane binding is considerably more complex, primarily because Si has substituents that change both electronic and steric properties, and the Si–H bond is more basic (better σ donor) than the H–H (and C–H) bonds.

4.2. Theoretical calculations and bonding model for silane coordination and activation

Calculations support a basically similar bonding picture for σ-silane complexes as to that for H_2 complexes, but with some differences. Early extended Hückel calculations in 1987 by Saillard on binding of SiH_4 to the $CpMn(CO)_2$ fragment showed that the Si–H overlap population is reduced to 0.24 by the σ(SiH) → M donation and M → σ*(SiH) BD, compared with 0.74 for uncoordinated SiH_4 [150]. Thus, the Si–H bond is weakened but not fully broken, and photoelectron spectroscopic studies show that the electronic structure of the interaction of $MeCpMn(CO)_2$ with $SiHPh_3$ is consistent with an early stage of X–H bond addition to M, and donation of X–H electrons to M predominates over BD [151–153]. As for H_2 coordination, there is a full range of M(SiH) interactions that span the extremes of complete OA to hardly any Si–H bond stretching. In most cases, however, the d_{MSi} remains relatively short regardless of the extent of activation, and there is no general explanation for this. On the other hand, the distance of the hydrogen from either the metal or Si can vary greatly; hence, the extent of bond activation is more problematic than for H_2 activation. A proposed trajectory for the reaction of silanes with the $CpMn(CO)_2$ fragment is illustrated below [132]:

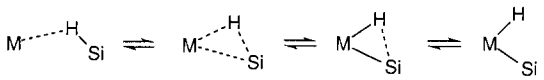

This also relates to H_2 binding and cleavage although the Si–H bond remains tilted throughout the OA process, but pivots so as to decrease d_{MSi} and to a lesser extent d_{MH} while the Si–H bond weakens and breaks. In the characterized silane complexes, the reaction coordinate seems arrested mostly in the middle to late

Table 8
J_{SiH} [a] for *cis*-Mo(η^2-H-SiHR$'_2$)(CO)($R_2PC_2H_4PR_2$)$_2$ and (MeCp)Mn(CO)(L)(η^2-H-SiR$'_3$)

complex	R or L	SiHR$'_2$	J_{SiH} (Hz) [b]	J_{SiH} (Hz) [c]
Mo	Et	SiH_3	35	164
	Et	SiH_2Ph	39	164, 170
	Et	$SiH_2(n\text{-}C_6H_{13})$	42	155, 168
	Et	$SiHPh_2$	50	172
	CH_2Ph	SiH_2Ph	41	164, 165
	CH_2Ph	$SiH_2(n\text{-}C_6H_{13})$	42	160, 166
	Ph	SiH_3	50	181
	Ph	SiH_2Ph	57	187, 194
	Ph	$SiH_2(n\text{-}C_6H_{13})$	61	180, 181
Mn	CO	$SiHPh_2$	63.5	205
	CN^nBu	$SiHPh_2$	57.5	194
	PPh_3	$SiHPh_2$	43	191
	PMe_3	$SiHPh_2$	38	188
	PMe_3	$SiCl_3$	20	
	CO	$SiCl_3$	54.8	

[a] Determined by $^1H\{^{31}P\}$- or ^{29}Si-NMR for Mo complexes [137,168] and Mn complexes [132], respectively.
[b] J_{SiH} for η^2-bound Si–H bonds.
[c] J_{SiH} for uncoordinated Si–H bonds.

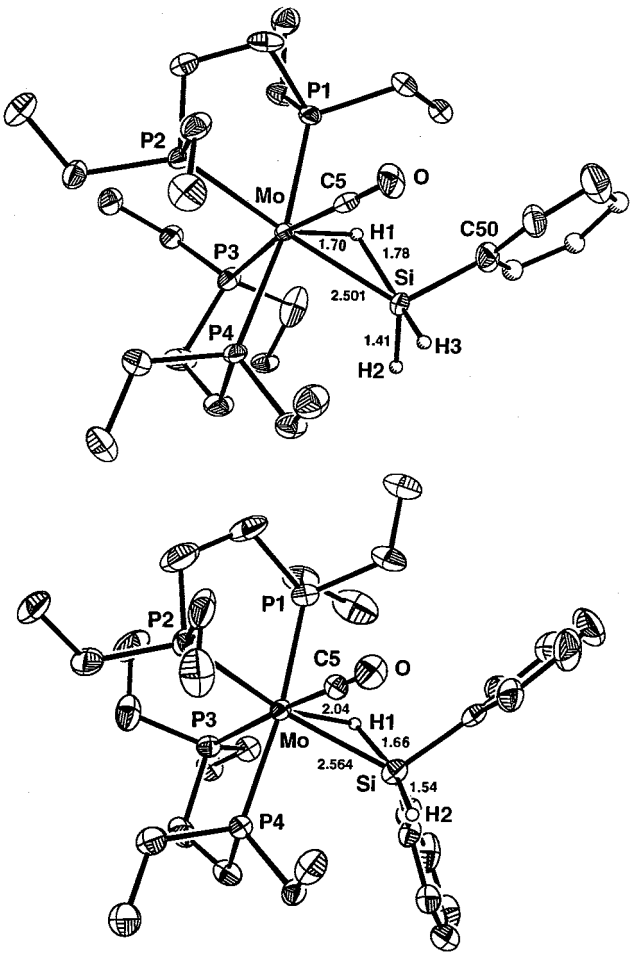

Fig. 7. ORTEP drawings of Mo(CO)(SiH_3Ph)(depe)$_2$ and the SiH_2Ph_2 analog.

part of this process where the d_{MSi} does not vary as much, although the fluctuation in experimental d_{MH} seems out of line.

The Si–H bond is more basic than either H–H or C–H and is probably a better σ donor to M according to Crabtree [135]. Also, the Si–H bond is weaker than H–H and C–H, hence a better π acceptor because the energy of the SiH σ* orbital is lower and is a better match with d-orbital energies. There is experimental evidence described below that silanes appear to be *both better σ-donors and π-acceptors* in comparison to H_2. Substituents at both M *and at Si* have large effects on the degree of activation towards OA and also on the reverse process, reductive elimination, i.e. silane dissociation [149,152,154]. Electron-withdrawing R groups on $HSiR_3$, such as Cl, increase Si–H activation and decrease J_{SiH} presumably because they lower the SiH σ* orbital energy, which favors increased BD. Withdrawing groups are also suggested to increase the s contribution in the Si orbital directed toward M, thereby increasing J_{SiH}, which opposes and diminishes the latter effect somewhat [132]. Electron-donating substituents such as alkyls decrease the Si–H activation and raise J_{SiH}, fostering σ coordination over OA. This is well illustrated in the products of silane reaction with the (MeCp)Mn(CO)(L) and Mo(CO)$(PP)_2$ fragments (Table 8). For the Mo system the activation of the Si–H bond is controlled by the electronic properties of both the R groups on the phosphine and the R′ groups on Si in opposing fashion, and a moderate J_{SiH} of 50 Hz is observed either for R = Et and R′ = Ph or R = Ph and R′ = H. The X-ray structures of Mo(CO)(SiH_2Ph_2)(depe)$_2$ and its SiH_3Ph analog (Fig. 7) have d_{SiH} of 1.66 and 1.77 Å, hence replacement of just one Ph by less donating H lengthens d_{SiH}, which correlates with a reduction in J_{SiH} from 50 to 39 Hz [155]. The lowest J_{SiH}, 35 Hz, is seen for the complex with the most electron-rich R (Et) and also for the least electron-rich R′ (i.e. for SiH_4), and the Si–H bond in SiH_4 is so activated that it undergoes equilibrium OA (Eq. (13)). The Mn complexes show similar behavior, and, as the donor strength of L increases down Table 8, J_{SiH} decreases. Therefore, although J_{SiH} can behave irregularly across a wide variety of complexes, it correlates well with electronic factors within a given system.

However, there are exceptions to the above: for interaction of silanes with strongly *electrophilic* fragments such as $Cr(CO)_5$, the binding energy *decreases* with more electron-withdrawing substituents on Si [156]. This reversal may reflect the relatively greater importance of SiH → M σ donation compared to BD for electrophilic M. Clearly the M–Si–H interaction can be finely tuned in several seemingly conflicting ways to give a series of complexes arrested along different points on the reaction coordinate to OA. Some paradoxical behavior is seen, e.g. W$(CO)_3(PR_3)_2$ oxidatively

adds silanes yet binds H_2 [44], which is opposite to the reactivity on more electron-rich $Mo(CO)(depe)_2$ (Eq. (15)).

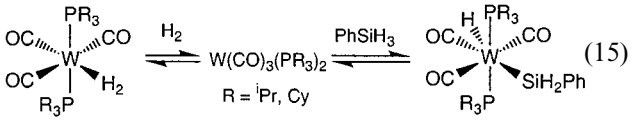

(15)

Thus there are subtle differences in H–H and Si–H activation. Although the *energetics of OA of silanes versus H_2 are comparable*, *whether the H–H or Si–H bond breaks more easily depends on the M/L system. For Group 6 systems*, *the H–H bond breaks suddenly when the electron richness of M is increased too much*, *e.g. changing R from Ph to Et in Eq. (16)*, *rather than elongating as for later metals.*

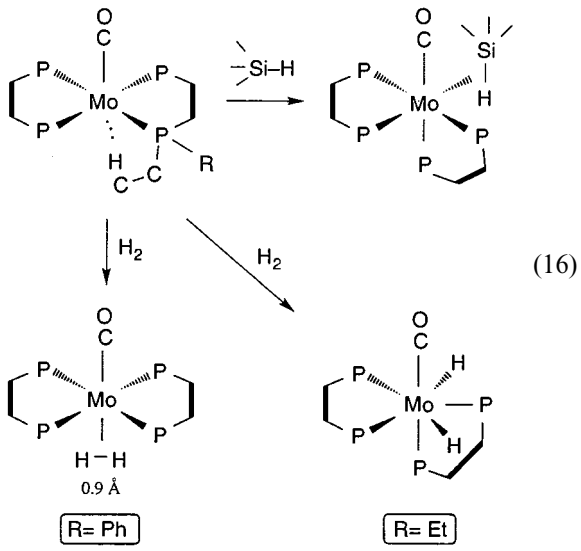

(16)

It is surprising that organosilanes do not oxidatively add to the Mo(CO)(depe)2 fragment that cleaves H_2 because silanes are better π-acceptors than H_2 and rearrange position to be *cis* to CO, ostensibly to avoid competing with CO for BD. Theoretical calculations on these and related silane complexes offer some insight on the bonding here [157], and a $Mo(CO)(PH_3)_4(H\cdots SiH_3)$ model also favors coordination of SiH_4 *cis* to CO for this electronic reason [157a]. The reversal of results compared to that for H_2 and $PhSiH_3$ addition to $W(CO)_3(PR_3)_2$ demonstrates the fine balance of electronic and steric forces here that may include structural rearrangement barriers for six- versus seven-coordination. For silane and σ ligands other than H_2, steric influences are magnified and perhaps favor the *cis*-(CO)(silane) orientation as well as disfavor OA to a seven-coordinate product with a silyl ligand that is quite large compared to a hydride.

The model complexes $Mo(CO)(L)(PH_3)_4$ ($L = H_2$, SiH_4) offer a good calculational comparison of Si–H and H–H bond activation, and the cis silane isomer is favored by 9.9 kcal over the *trans* isomer where the silane competes with CO for BD [157a]. The optimized *cis* structure shows a d_{SiH} of 1.813 Å close to the experimental value of 1.77 Å in *cis*-$Mo(CO)(depe)_2(SiH_2Ph_2)$. Analysis of the electron density around the Mo(H···Si) triangle shows significant differences compared to the situation for true (unstretched) H_2 coordination. A covalent-type Mo–Si bond is indicated by one local concentration for both Mo and Si while the Mo–H bond is essentially a dative $H^- \rightarrow Mo$ interaction similar to $P \rightarrow Mo$. The bond path of H···S is curved inward with the turning point sloped toward Si, implying that the H–Si covalent bond is significantly weakened.

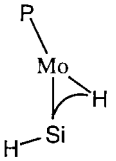

In true $M–H_2$ coordination, the H–H covalent bonding is retained for the most part, i.e. there is higher electron density between the two H and less $M \rightarrow H_2$ BD than $H_2 \rightarrow M$ σ donation. However, for the silane bonding here, the situation is more like stretched H_2 complexes because silanes are stronger π-acceptors than H_2. There are large degrees of density concentrations in both Mo–H and Mo–Si bonds, although there is still appreciable concentration between H and Si. Thus silane complexes lie closer to the OA product than H_2 complexes, as depicted below, and true nonclassical Si–H interactions occur primarily for highly electrophilic centers, d^0 systems where BD is weak, or β-agostic systems.

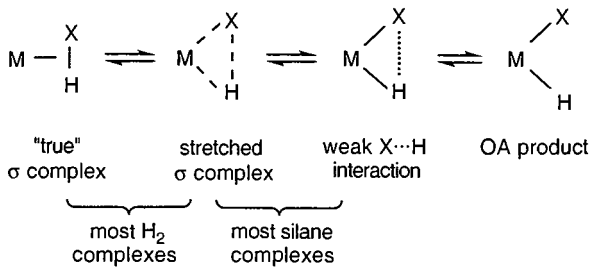

Fan et al. conclude that the hydrogen in $M(H)(SiR_3)$ is more hydridic than in MH_2 and that its attraction to Si to form stretched σ complexes is facilitated by the ease of Si to become hypervalent with an adjacent electronegative ligand [157a]. However, the similarity in the overall reaction coordinate for OA of H–H and Si–H bonds indicates that the bonding situation is not vastly different, but mainly that *M–silane interactions are arrested further along the reaction coordinate and steric factors are more important.*

Summarizing, there are at least five primary variables in $L_nM(\eta^2\text{-}X–H)$ systems influencing the electronics and hence activation towards OA: the nature of M and X, the substituents at both M and X, and also L,

especially when *trans* to XH (X = C, Si, Ge, etc.). Additionally, steric factors and overall energetics of OA processes could play important roles in determining the point at which a σ bond breaks. Silanes bind less easily than the diminutive H_2 ligand to smaller first row metals with bulky phosphines. This is counterbalanced somewhat by fact that H–SiR_3 ligands are both better σ-donors and π-acceptors than H_2 and can approach M in tilted fashion with the H atom in front and the bulky SiR_3 out of the way. The binding and activation of σ bonds other than H_2 will always be much more complex electronically and sterically and even lead to counterintuitive behavior. Although the reaction coordinates for H–H and Si–H bond cleavage are quite similar in most aspects, the stronger σ-acceptor strength of the Si–H bond often leads to σ complexes arrested further along the reaction coordinate towards OA than for H_2 binding.

5. σ Complexes of boranes: a different type of backbonding

Although borohydride ligands (BH_4^- and related $B_xH_y^{n-}$ species) are well known, they bear negative charge and to more clearly define the bonding and properties of a true σ B–H complex, a *neutral* ligand coordinated only by an M–B–H linkage is needed. Neutral boranes such as BH_3 are Lewis acids but their base adducts such as $BH_3{\cdot}PR_3$ are potential σ ligands more analogous to silanes than the negatively charged borohydrides. The X-ray structures of Group 6 pentacarbonyl analogs such as $W(CO)_5(BH_3{\cdot}PMe_3)$ clearly show monodentate η^2-B–H coordination [158].

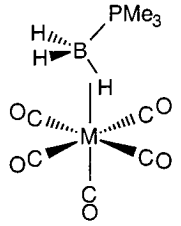

M = Cr, W

30

Compound **30** is among the first examples of intermolecular coordination of a single B–H bond in a neutral borane to a transition metal, and all of these species can be regarded as models for alkane coordination. The crystal structures of borane complexes such as **30** are of interest to compare with those for other octahedral σ complexes, particularly silane complexes. The d_{BH} (1.1–1.3 Å) are not well determined (large standard deviations) and are not very meaningful. The M–H–B angles in $M(CO)_5(BH_3{\cdot}PMe_3)$ are near 130° (again with large estimated standard deviations) and can be as high as 167° in related systems. These are much larger than the angles observed in M–H–Si σ complexes and the Ti(HBcat) σ complexes discussed below. Thus, the bonding for these neutral borane ligands, while still bent, is closer to end-on than side-on as in borohydride complexes where M–H–B can be as high as 162°. Because these borane ligands contain four-coordinate boron when free, they are more like BH_4^- complexes even though they are neutral. There is certainly more hydridic character than in the base-free catecholboranes discussed below. It is clear that d_{BH} vary unpredictably, and the M–H–B angles perhaps also lack sufficient accuracy. However, d_{MB} is meaningful and is much longer, by ~0.6 Å, in $W(CO)_5(BH_3{\cdot}PMe_3)$ than in $Cp_2W(BR_2)$ which has direct W–B bonds [159]. This would suggest that the electron density in the B–H bond being donated to M resides closer to H than B (see below for discussion of bonding).

Titanocene catecholborane complexes (**31**) recently synthesized and characterized by Hartwig appear to the best examples of genuine η^2-BH σ complexes [160–162].

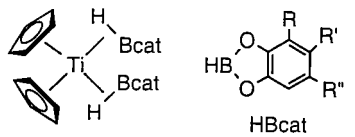

31

The Hbcat ligand is neutral with three-coordinate boron, and the asymmetric side-on bonding geometry with Ti–H–B near 100° (Fig. 8) is more like that in η^2-silanes than that in the borohydrides or $W(CO)_5(BH_3{\cdot}PMe_3)$. The values of d_{MB} (2.335(5) Å) in **31** are longer than in metallocene boryl complexes, indicative of a bond order of less than one, but are significantly shorter than in the $M(CO)_5(BH_3{\cdot}PMe_3)$ species. The value of d_{TiH} of 1.74(4) Å is relatively short indicating substantial interaction. The most striking feature of the structure of **31** is the unusual geometry about boron, which has bonding interactions to four other atoms. The sum of the three angles at B that do not include H is 360°, indicating that the Ti, two oxygens, and B all lie in the same plane, i.e. the boron is highly distorted from tetrahedral geometry.

Theoretical studies of model complexes give insight into the nature of the M(η^2-BH) bonding in **31**, which differs substantially from that in other σ complexes [160,163,164]. In an ab initio study of hydride exchange processes in $OsH_3(BH_4)(PR_3)_2$, an intermediate with a η^2-BH_3 ligand is stable by theoretical calculations, although such a species is not known experimentally [163].

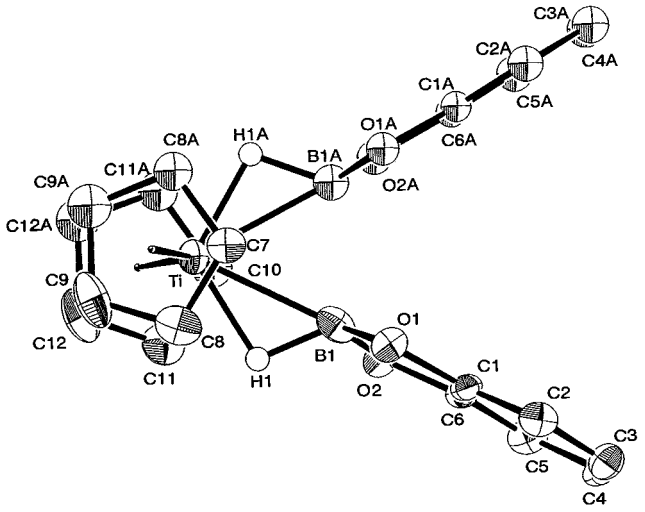

Fig. 8. ORTEP drawing of $Cp_2Ti(HBcat)_2$.

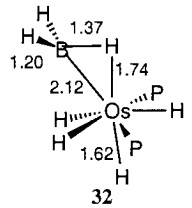

32

The M–H–B angle of 85° in **32** is slightly more acute than that in silane complexes. Donation from the B–H bond to M occurs, but unlike for most other σ complexes, *BD from M does not go to the σ* B–H orbital but rather to a boron pπ orbital that is nonbonding with the hydrogen atom*. Importantly, this interaction would not be expected to promote breaking the B–H bond in an OA process. The geometry is also unusual in that it looks like an H bridging a BH_2 group and Os, i.e. the two H atoms bend away from M instead of keeping BH_3 trigonal planar.

Calculations on $Cp_2Ti[HB(OH)_2]_2$ models for **31** verify the above bonding situation and also indicate a 3c–2e bond involving the B–Ti–B triangle [160,164]. There is overlap between the borons, which are close together ($d_{BB} = 2.11$ Å). Hartwig et al. show that BD from Ti again goes into boron p-orbitals (shown in **33**), which are lower in energy than the σ* orbitals of X–H bonds in general. Lin's representation (**34**) shows that the major interaction involves a filled Ti $1a_1$ orbital and the in-phase combination of the two empty sp^3-hybridized orbitals from the $HB(OH)_2$ units. Both cases

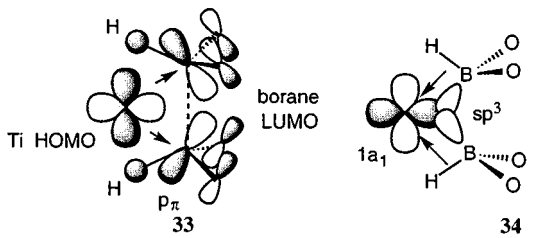

give a closer energy match with the d-orbitals and hence a stronger BD interaction than in other σ complexes. Equilibrium studies show that HBcat binding is thermodynamically favored over silane binding here, partly because the borane is more Lewis acidic and enhances BD (HBcat forms adducts with amines whereas $SiHPh_3$ does not). Furthermore, invoking this BD explains the unusual geometry at B also seen in the Os complex: maximum overlap exists when the Ti, B, and O atoms are coplanar. The complete series of complexes $Cp_2Ti(HBcat)(L)$ may be viewed as being additionally stabilized by some degree of intramolecular interaction with boron such as the B···B interaction above and B···H and B···C interactions in the silane (**35**) and alkyne (**36**) species that undoubtedly facilitate hydrogen exchange and hydroboration.

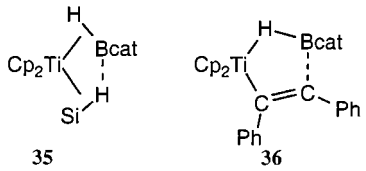

In terms of the influence of the electronic nature of L only, the stabilities follow the usual trends: donors such as PR_3 stabilize the complexes and CO destabilizes. Finally, as for silanes the stability of the σ complexes depends on the substituents on B, in this case the substituents R, R′, and R″ on the catechol aromatic ring. The rates for borane dissociation decrease with increasingly electron-withdrawing R groups, just as such groups on R_3SiH give more activated M(Si–H) bonds and more stable complexes.

In summary, coordination and activation of B–H bonds closely parallels other M σ bond interactions. The bonding is clearly 3c–2e, giving bent M–H–B geometries. As for M–silane and other metal σ bond interactions, there are several degrees of activation of the B–H bond (forms **37**–**39**) [165].

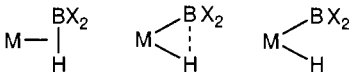

However there are notable differences, and the variables of charge and coordination number for boron come into play and cloud the comparisons. Structural and spectroscopic gauges such as d_{BH} and J_{BH} are not as well defined or available as for H–H and Si–H activation. The most significant difference appears to be the nature of M → borane BD for certain systems where a pπ orbital on boron is lower in energy than B–H σ* and receives BD. Theoretical studies of OA of $(HO)_2B–XH_3$ to $Pt(PH_3)_2$ (X = C, Si, etc.) show that the σ B–X complex in the transition state is highly

stabilized by the charge-transfer interaction between a metal d-orbital and a $B(OH)_2$ p-orbital (as in **33**) and is the main reason for the high reactivity of $(HO)_2B–XH_3$ in the OA reaction [166]. OA occurs with moderate activation energy for X = C and with either a very small or no barrier for X = Ge, Si, and Sn. Further studies are needed to resolve the mechanism of OA of B–X, which differs both by theoretical calculations and experimentally from that of other OA processes.

Acknowledgements

This work was supported by the Department of Energy, Office of Basic Energy Sciences, Chemical Sciences Division. The author is grateful to his colleagues and collaborators at Los Alamos, especially Juergen Eckert and Jeff Hay, for their seminal development of the experimental and theoretical evidence for $M \rightarrow H_2$ backdonation in $W(CO)_3(PR_3)_2(H_2)$ and related Group 6 complexes.

References

[1] (a) G.J. Kubas, Acc. Chem. Res. 21 (1988) 120;
(b) G.J. Kubas, Metal Dihydrogen and σ-Bond Complexes, Kluwer Academic/Plenum Press, New York, 2001.
[2] M. Elian, M.M.L. Chen, D.M.P. Mingos, R. Hoffmann, Inorg. Chem. 15 (1976) 1148.
[3] (a) M.J.S. Dewar, Bull. Soc. Chim. Fr. 18 (1951) C79;
(b) J. Chatt, L.A. Duncanson, J. Chem. Soc. (1953) 2929;
(c) Recent experimental verification: L. Triguero, A. Fohlisch, P. Vaterlein, J. Hasselstrom, M. Weinelt, L.G.M. Pettersson, Y. Luo, H. Agren, A. Nilsson, J. Am. Chem. Soc. 122 (2000) 12310.
[4] T. Hasegawa, Z. Li, S. Parkin, H. Hope, R.K. McMullan, T.F. Koetzle, H. Taube, J. Am. Chem. Soc. 116 (1994) 4352.
[5] M.A. Andrews, S.W. Kirtley, H.D. Kaesz, Adv. Chem. Ser. 167 (1978) 229.
[6] H.J. Wasserman, G.J. Kubas, R.R. Ryan, J. Am. Chem. Soc. 108 (1986) 2294.
[7] (a) F.A. Cotton, A.G. Stanislowski, J. Am. Chem. Soc. 96 (1974) 5074;
(b) F.A. Cotton, V.W. Day, J. Chem. Soc. Chem. Commun. (1974) 415.
[8] M. Brookhart, M.L.H. Green, L.-L. Wong, Prog. Inorg. Chem. 36 (1988) 1.
[9] J.-Y. Saillard, R. Hoffmann, J. Am. Chem. Soc. 106 (1984) 2006.
[10] S. Geftakis, G.E. Ball, J. Am. Chem. Soc. 120 (1998) 9953.
[11] P.J. Brothers, Prog. Inorg. Chem. 28 (1981) 1.
[12] M.Y. Darensbourg, E.J. Lyon, J.J. Smee, Coord. Chem. Rev. 206–207 (2000) 533.
[13] A.M. Joshi, K.S. MacFarlane, B.R. James, J. Organomet. Chem. 488 (1995) 161.
[14] G. Jia, W.S. Ng, C.P. Lau, Organometallics 17 (1998) 4538.
[15] P.G. Jessop, R.H. Morris, Coord. Chem. Rev. 121 (1992) 155.
[16] R.H. Morris, Can. J. Chem. 74 (1996) 1907.
[17] (a) T.P. Fong, A.J. Lough, R.H. Morris, A. Mezzetti, E. Rocchini, P. Rigo, J. Chem. Soc. Dalton Trans. (1998) 2111;
(b) T.P. Fong, C.E. Forde, A.J. Lough, R.H. Morris, P. Rigo, E. Rocchini, T. Stephan, J. Chem. Soc. Dalton Trans. (1999) 4475;
(c) A.C. Ontko, J.F. Houlis, R.C. Schnabel, D.M. Roddick, T.P. Fong, A.J. Lough, R.H. Morris, Organometallics 17 (1998) 5467.
[18] (a) M.S. Chinn, D.M. Heinekey, N.G. Payne, C.D. Sofield, Organometallics 8 (1989) 1824;
(b) J. Huhmann-Vincent, B.L. Scott, G.J. Kubas, Inorg. Chim. Acta 294 (1999) 240;
(c) J. Huhmann-Vincent, B.L. Scott, G.J. Kubas, J. Am. Chem. Soc. 120 (1998) 6808.
[19] (a) R. Kuhlman, Coord. Chem. Rev. 167 (1997) 205;
(b) E.T. Papish, F. Rix, N. Spetseris, J.R. Norton, R.D. Williams, J. Am. Chem. Soc. 122 (2000) 12235.
[20] X. Fang, J. Huhmann-Vincent, B.L. Scott, G.J. Kubas, J. Organomet. Chem. 609 (2000) 95.
[21] D. Marx, M. Parrinello, Nature 375 (1995) 216.
[22] A.G. Ginsburg, A.A. Bagaturyants, Organomet. Chem. USSR 2 (1989) 111.
[23] C.A. Tsipis, Coord. Chem. Rev. 108 (1991) 163.
[24] Z. Lin, M.B. Hall, Coord. Chem. Rev. 135/136 (1994) 845.
[25] A. Dedieu (Ed.), Transition Metal Hydrides, VCH Publishers, New York, 1992.
[26] (a) P.W.N.M. van Leeuwen, K. Morokuma, J.H. van Lenthe (Eds.), Theoretical Aspects of Homogeneous Catalysis, Kluwer Academic, Boston, 1995;
(b) D.G. Musaev, K. Morokuma, Adv. Chem. Phys. 95 (1996) 61.
[27] (a) F. Maseras, A. Lledos, E. Clot, O. Eisenstein, Chem. Rev. 100 (2000) 601;
(b) S. Niu, M.B. Hall, Chem. Rev. (2000) 353;
(c) A. Dedieu, Chem. Rev. (2000) 543; G. Frenking, N. Fröhlich, Chem. Rev. (2000) 717;
(d) M. Torrent, M. Solà, G. Frenking, Chem. Rev. (2000) 439.
[28] G.J. Kubas, R.R. Ryan, B.I. Swanson, P.J. Vergamini, H.J. Wasserman, J. Am. Chem. Soc. 106 (1984) 451.
[29] R.G. Parr, W. Yang, Density Functional Theory of Atoms and Molecules, Oxford University Press, Oxford, 1989.
[30] A. Dedieu, A. Strich, Inorg. Chem. 18 (1979) 2940.
[31] R.H. Crabtree, J.M. Quirk, J. Organomet. Chem. 199 (1980) 99.
[32] S.A. Macgregor, O. Eisenstein, M.K. Whittlesey, R.N. Perutz, J. Chem. Soc. Dalton Trans. (1998) 291 (and references therein).
[33] T. Ziegler, V. Tschinke, L. Fan, A.D. Becke, J. Am. Chem. Soc. 111 (1989) 9177.
[34] (a) A.A. Bagatur'yants, O.V. Gritsenko, G.M. Zhidomirov, Russ. J. Phys. Chem. 54 (1980) 2993;
(b) O.V. Gritsenko, A.A. Bagatur'yants, I.I. Moiseev, V.B. Kazanskii, I.V. Kalechits, Kinet. Katal. 21 (1980) 632 (see also 22 (1981) 354).
[35] A.A. Bagatur'yants, N.A. Anikin, G.M. Zhidomirov, V.B. Kazanskii, Russ. J. Phys. Chem. 55 (1981) 1157.
[36] H. Nakatsuji, M. Hada, Croat. Chem. Acta 57 (1984) 1371.
[37] (a) M.R.A. Blomberg, U.B. Brandemark, L.G.M. Petterson, P.E.M. Siegbahn, Int. J. Quantum Chem. 23 (1983) 855;
(b) U.B. Brandemark, M.R.A. Blomberg, L.G.M. Petterson, P.E.M. Siegbahn, J. Phys. Chem. 88 (1984) 4617.
[38] C. Jarque, O. Novaro, M.E. Ruiz, J. Garcia-Prieto, J. Am. Chem. Soc. 108 (1986) 3507.
[39] (a) J.J. Low, W.A. Goddard III, J. Am. Chem. Soc. 106 (1984) 8321;
(b) J.J. Low, W.A. Goddard III, Organometallics 5 (1986) 609;
(c) H. Nakatsuji, M. Hada, T. Yonezawa, J. Am. Chem. Soc. 109 (1987) 1902;
(d) K. Balasubramanian, Chem. Phys. 88 (1988) 6955.

[40] G.A. Ozin, J. Garcia-Prieto, J. Am. Chem. Soc. 108 (1986) 3099.
[41] (a) L. Andrews, L. Manceron, M.E. Alikhani, X. Wang, J. Am. Chem. Soc. 122 (2000) 11011;
(b) L. Andrews, X. Wang, M.E. Alikhani, L. Manceron, J. Phys. Chem. A 105 (2001) 3052.
[42] (a) P.J. Hay, Chem. Phys. Lett. 103 (1984) 466;
(b) P.J. Hay, J. Am. Chem. Soc. 109 (1987) 705;
(c) J. Eckert, G.J. Kubas, J.H. Hall, P.J. Hay, C.M. Boyle, J. Am. Chem. Soc. 112 (1990) 2324.
[43] (a) J. Tomas, A. Lledos, Y. Jean, Organometallics 17 (1998) 190;
(b) J. Tomas, A. Lledos, Y. Jean, Organometallics 17 (1998) 4932;
(c) J. Li, T. Ziegler, Organometallics 15 (1996) 3844.
[44] M.D. Butts, G.J. Kubas, X.-L. Luo, J.C. Bryan, Inorg. Chem. 36 (1997) 3341.
[45] D.M. Heinekey, C.E. Radzewich, M.H. Voges, B.M. Schomber, J. Am. Chem. Soc. 119 (1997) 4172.
[46] R.R. Andrea, M.A. Vuurman, D.J. Stufkens, A. Oskam, Recl. Trav. Chim. Pays-Bas 105 (1986) 372.
[47] Y. Ishikawa, P.A. Hackett, D.M. Rayner, J. Phys. Chem. 93 (1989) 652.
[48] H.J. Wasserman, G.J. Kubas, R.R. Ryan, J. Am. Chem. Soc. 108 (1986) 2294.
[49] T. Tatsumi, H. Tominaga, M. Hidai, Y. Uchida, J. Organomet. Chem. 199 (1980) 63.
[50] G.J. Kubas, C.J. Burns, J. Eckert, S. Johnson, A.C. Larson, P.J. Vergamini, C.J. Unkefer, G.R.K. Khalsa, S.A. Jackson, O. Eisenstein, J. Am. Chem. Soc. 115 (1993) 569.
[51] G.J. Kubas, R.R. Ryan, C.J. Unkefer, J. Am. Chem. Soc. 109 (1987) 8113.
[52] (a) W.A. Schenk, F.-E. Baumann, Chem. Ber. 115 (1982) 2615;
(b) M.A. Graham, M. Poliakoff, J.J. Turner, J. Chem. Soc. A (1979) 2939;
(c) R.A. Brown, G.R. Dobson, Inorg. Chem. Acta 6 (1972) 65;
(d) I.W. Stolz, G.R. Dobson, R.K. Sheline, Inorg. Chem. 2 (1963) 1264.
[53] R.N. Perutz, J.J. Turner, Inorg. Chem. 18 (1979) 2940.
[54] J. Li, T. Ziegler, Organometallics 15 (1996) 3844.
[55] S. Dapprich, G. Frenking, Angew. Chem. Int. Ed. Engl. 34 (1995) 354.
[56] S. Dapprich, G. Frenking, Z. Anorg. Allg. Chem. 624 (1998) 583.
[57] (a) S. Dapprich, G. Frenking, Organometallics 15 (1996) 4547;
(b) G. Frenking, U. Pidum, J. Chem. Soc. Dalton Trans. (1997) 1653.
[58] F.M. Bickelhaupt, E.J. Baerends, W. Ravenek, Inorg. Chem. 29 (1990) 350.
[59] J. Li, R.M. Dickson, T. Ziegler, J. Am. Chem. Soc. 117 (1995) 11482.
[60] F. Maseras, X.-K. Li, N. Koga, K. Morokuma, J. Am. Chem. Soc. 115 (1993) 10974.
[61] A. Toupadakis, G.J. Kubas, W.A. King, B.L. Scott, J. Huhmann-Vincent, Organometallics 17 (1998) 5315.
[62] U. Radius, F.M. Bickelhaupt, A.W. Ehlers, N. Goldberg, R. Hoffmann, Inorg. Chem. 37 (1998) 1080.
[63] (a) A.W. Ehlers, Y. Ruiz-Morales, E.J. Baerends, T. Ziegler, Inorg. Chem. 36 (1997) 5031;
(b) A.J. Lupinetti, S. Fau, G. Frenking, S.H. Strauss, J. Phys. Chem. 101 (1997) 9551.
[64] (a) R.K. Szilagyi, G. Frenking, Organometallics 16 (1997) 4807;
(b) A. Diefenbach, F.M. Bickelhaupt, G. Frenking, J. Am. Chem. Soc. 122 (2000) 6449.
[65] T. Ishida, Y. Mizobe, T. Tanase, M. Hidai, J. Organomet. Chem. 409 (1991) 355.
[66] B.J. Coe, S.J. Glenwright, Coord. Chem. Rev. 203 (2000) 5.
[67] A. Albinati, V.I. Bakhmutov, K.G. Caulton, E. Clot, J. Eckert, O. Eisenstein, D.G. Gusev, V.V. Grushin, B.E. Hauger, W.T. Klooster, T.F. Koetzle, R.K. McMullan, T.J. O'Loughlin, M. Pelissier, J.S. Ricci, M.P. Sigalas, A.B. Vymenits, J. Am. Chem. Soc. 115 (1993) 7300.
[68] M. Schlaf, A.J. Lough, P.A. Maltby, R.H. Morris, Organometallics 15 (1996) 2270 (and references therein).
[69] W.A. King, B.L. Scott, J. Eckert, G.J. Kubas, Inorg. Chem. 38 (1999) 1069.
[70] C.E. Forde, S.E. Landau, R.H. Morris, J. Chem. Soc. Dalton Trans. (1997) 1663.
[71] P.J. Hay, unpublished data.
[72] (a) T. Pang, Chem. Phys. Lett. 228 (1994) 555;
(b) M. Farizon, B. Farizon-Mazuy, N.V. de Castro Faria, H. Chermette, Chem. Phys. Lett. 177 (1991) 451.
[73] B.R. Bender, G.J. Kubas, L.H. Jones, B.I. Swanson, J. Eckert, K.B. Capps, C.D. Hoff, J. Am. Chem. Soc. 119 (1997) 9179.
[74] F. Maseras, A. Lledos, M. Costas, J.M. Poblet, Organometallics 15 (1996) 2947.
[75] I. Bytheway, G.B. Bacskay, N.S. Hush, J. Phys. Chem. 110 (1996) 6023.
[76] I. Bytheway, I. Craw, G.B. Bacskay, N.S. Hush, Adv. Chem. Ser. 253 (1997) 21.
[77] J.S. Craw, G.B. Bacskay, N.S. Hush, J. Am. Chem. Soc. 116 (1994) 5937.
[78] (a) R. Gelabert, M. Moreno, J.M. Lluch, A. Lledos, J. Am. Chem. Soc. 119 (1997) 9840 (see also 120 (1998) 8168);
(b) L. Torres, R. Gelabert, M. Moreno, J.M. Lluch, J. Phys. Chem. A 104 (2000) 7898.
[79] (a) G. Barea, M.A. Esteruelas, A. Lledos, A.M. Lopez, E. Onate, J.I. Tolosa, Organometallics 17 (1998) 4065;
(b) G. Barea, M.A. Esteruelas, A. Lledos, A.M. Lopez, J.I. Tolosa, Inorg. Chem. 37 (1998) 5033;
(c) J.S. Craw, G.B. Backsay, N.S. Hush, Inorg. Chem. 32 (1993) 2230.
[80] P.A. Maltby, M. Schlaf, M. Steinbeck, A.J. Lough, R.H. Morris, W.T. Klooster, T.F. Koetzle, R.C. Srivastava, J. Am. Chem. Soc. 118 (1996) 5396.
[81] W.T. Klooster, T.F. Koetzle, G. Jia, T.P. Fong, R.H. Morris, A. Albinati, J. Am. Chem. Soc. 116 (1994) 7677.
[82] C.A. Bayse, M.B. Hall, B. Pleune, R. Poli, Organometallics 17 (1998) 4309.
[83] B. Chaudret, G. Chung, O. Eisenstein, S.A. Jackson, F.J. Lahoz, J.A. Lopez, J. Am. Chem. Soc. 113 (1991) 2314.
[84] L.S. Van Der Sluys, J. Eckert, O. Eisenstein, J.H. Hall, J.C. Huffman, S.A. Jackson, T.F. Koetzle, G.J. Kubas, P.J. Vergamini, K.G. Caulton, J. Am. Chem. Soc. 112 (1990) 4831.
[85] (a) S.A. Jackson, O. Eisenstein, J. Am. Chem. Soc. 112 (1990) 7203;
(b) J.-F. Riehl, M. Pelissier, O. Eisenstein, Inorg. Chem. 31 (1992) 3344.
[86] B. Chaudret, G. Chung, O. Eisenstein, S.A. Jackson, F.J. Lahoz, J.A. Lopez, J. Am. Chem. Soc. 113 (1991) 2314.
[87] F. Maseras, M. Duran, A. Lledos, J. Bertran, J. Am. Chem. Soc. 113 (1991) 2879.
[88] C. Bianchini, D. Masi, M. Peruzzini, M. Casarin, C. Maccato, G.A. Rizzi, Inorg. Chem. 36 (1997) 1061.
[89] V. Rodriguez, S. Sabo-Etienne, B. Chaudret, J. Thoburn, S. Ulrich, H.-H. Limbach, J. Eckert, J.-C. Barthelat, K. Hussein, C.J. Marsden, Inorg. Chem. 37 (1998) 3475.
[90] C. Soubra, F. Chan, T.A. Albright, Inorg. Chim. Acta 272 (1998) 95.
[91] A.F. Borowski, B. Donnadieu, J.-C. Daran, S. Sabo-Etienne, B. Chaudret, Chem. Commun. (2000) 543.
[92] H.H. Brintzinger, J. Organomet. Chem. 171 (1979) 337.
[93] J.K. Burdett, J.R. Phillips, M.R. Pourian, M. Poliakoff, J.J. Turner, R. Upmacis, Inorg. Chem. 26 (1987) 3054.

[94] (a) J.K. Burdett, M.R. Pourian, Organometallics 6 (1987) 1684; (b) J.K. Burdett, M.R. Pourian, Inorg. Chem. 27 (1988) 4445.
[95] X.-L. Luo, R.H. Crabtree, J. Am. Chem. Soc. 112 (1990) 6912.
[96] F. Maseras, M. Duran, A. Lledos, J. Bertran, J. Am. Chem. Soc. 114 (1992) 2922.
[97] D.G. Gusev, R. Hubener, P. Burger, O. Orama, H. Berke, J. Am. Chem. Soc. 119 (1997) 3716.
[98] M.E. Thompson, S.M. Baxter, A.R. Bulls, B.J. Burger, M.C. Nolan, B.D. Santarsiero, W.P. Schaefer, J.E. Bercaw, J. Am. Chem. Soc. 109 (1987) 203.
[99] P.L. Watson, G.W. Parshall, Acc. Chem. Res. 18 (1985) 51.
[100] G. Jeske, H. Lauke, H. Mauermann, H. Schumann, T.J. Marks, J. Am. Chem. Soc. 107 (1985) 8111.
[101] C.S. Christ Jr., J.R. Eyler, D.E. Richardson, J. Am. Chem. Soc. 110 (1988) 4038 (see also 112 (1990) 596).
[102] Theoretical analyses: (a) S. Niu, M.B. Hall, Chem. Rev. 100 (2000) 353;
(b) H.H. Brintzinger, J. Organomet. Chem. 171 (1979) 337;
(c) H. Rabaa, J.-Y. Saillard, R. Hoffmann, J. Am. Chem. Soc. 108 (1986) 4327;
(d) M.L. Steigerwald, W.A. Goddard III, J. Am. Chem. Soc. 106 (1984) 308; A.K. Rappe, Organometallics 9 (1990) 466;
(e) A. Dedieu, F. Hutschka, A. Milet, ACS Symp. Ser., vol. 721(Transition State Modeling for Catalysis), 1999, pp. 100–113;
(f) A. Milet, A. Dedieu, G. Kapteijn, G. van Koten, Inorg. Chem. 36 (1997) 3223;
(g) E. Folga, T. Ziegler, Can. J. Chem. 70 (1992) 333;
(h) T. Ziegler, E. Folga, A. Berces, J. Am. Chem. Soc. 115 (1993) 636;
(i) L. Versluis, T. Ziegler, Organometallics 9 (1990) 2985; M. Sola, T. Ziegler, Organometallics 15 (1996) 2611;
(j) Y. Musashi, S. Sakaki, J. Am. Chem. Soc. 122 (2000) 3867;
(k) L. Maron, O. Eisenstein, J. Am. Chem. Soc. 123 (2001) 1036.
[103] J. Eckert, G.J. Kubas, A.J. Dianoux, J. Chem. Phys. 88 (1988) 466.
[104] J. Eckert, H. Blank, M.T. Bautista, R.H. Morris, Inorg. Chem. 29 (1990) 747.
[105] J. Eckert, Spectrochim. Acta 48A (1992) 363.
[106] J. Eckert, G.J. Kubas, J. Chem. Phys. 97 (1993) 2378.
[107] J. Eckert, Trans. Am. Crystallogr. Assoc. 31 (1997) 45.
[108] E. Clot, J. Eckert, J. Am. Chem. Soc. 121 (1999) 8855.
[109] (a) G. Barea, M.A. Esteruelas, A. Lledos, A.M. Lopez, E. Onate, J.I. Tolosa, Organometallics 17 (1998) 4065;
(b) R. Gelabert, M. Moreno, J.M. Lluch, A. Lledos, J. Am. Chem. Soc. 120 (1998) 8168.
[110] (a) K.W. Zilm, R.A. Merrill, M.W. Kummer, G.J. Kubas, J. Am. Chem. Soc. 108 (1986) 7837;
(b) K.W. Zilm, J.M. Millar, Adv. Magn. Opt. Reson. 15 (1990) 163.
[111] I.F. Silvera, Rev. Mod. Phys. 52 (1980) 393.
[112] J.P. Beaufils, T. Crowley, R.K. Rayment, R.K. Thomas, J.W. White, Mol. Phys. 44 (1981) 1257.
[113] J.M. Nicol, J. Eckert, J. Howard, J. Phys. Chem. 92 (1988) 7117.
[114] M. Prager, A. Heidemann, Chem. Rev. 97 (1997) 2933.
[115] J. Eckert, Physica B 136 (1986) 150.
[116] J. Eckert, G.J. Kubas, R.P. White, Inorg. Chem. 31 (1992) 1550.
[117] G.J. Kubas, J.E. Nelson, J.C. Bryan, J. Eckert, L. Wisniewski, K. Zilm, Inorg. Chem. 33 (1994) 2954.
[118] G.E. Gadd, R.K. Upmacis, M. Poliakoff, J.J. Turner, J. Am. Chem. Soc. 108 (1986) 2547.
[119] R.K. Upmacis, M. Poliakoff, J.J. Turner, J. Am. Chem. Soc. 108 (1986) 3645.
[120] R.L. Sweany, J. Am. Chem. Soc. 107 (1990) 2374.
[121] Y. Jean, O. Eisenstein, F. Volatron, B. Maouche, F. Sefta, J. Am. Chem. Soc. 108 (1986) 6587.
[122] J. Eckert, A. Albinati, R.P. White, C. Bianchini, M. Peruzzini, Inorg. Chem. 31 (1992) 4241.
[123] J. Eckert, A. Albinati, U.E. Bucher, L.M. Venanzi, Inorg. Chem. 35 (1996) 1292.
[124] (a) J. Eckert, C.M. Jensen, G. Jones, E. Clot, O. Eisenstein, J. Am. Chem. Soc. 115 (1993) 11056;
(b) J. Eckert, C.M. Jensen, T.F. Koetzle, T. Le-Husebo, J. Nicol, P. Wu, J. Am. Chem. Soc. 117 (1995) 7271.
[125] S. Li, M.B. Hall, J. Eckert, C.M. Jensen, A. Albinati, J. Am. Chem. Soc. 122 (2000) 2903.
[126] R. Gelabert, M. Moreno, J.M. Lluch, A. Lledos, Organometallics 16 (1997) 3805.
[127] R.H. Morris, Inorg. Chem. 31 (1992) 1471.
[128] (a) A.B.P. Lever, Inorg. Chem. 29 (1990) 1271;
(b) A.B.P. Lever, Inorg. Chem. 30 (1991) 1980.
[129] A. Antinolo, F. Carrillo-Hermosilla, M. Fajardo, S. Garcia-Yuste, A. Otero, S. Camanyes, F. Maseras, M. Moreno, A. Lledos, J.M. Lluch, J. Am. Chem. Soc. 119 (1997) 6107.
[130] F.A. Jalon, A. Otero, B.R. Manzano, E. Villasenor, B. Chaudret, J. Am. Chem. Soc. 117 (1995) 10123.
[131] (a) S. Sabo-Etienne, B. Chaudret, H. Abou el Makarim, J.-C. Barthelet, J.-C. Daudey, S. Ulrich, H.-H. Limbach, C. Moise, J. Am. Chem. Soc. 117 (1995) 11602;
(b) S. Sabo-Etienne, V. Rodriguez, B. Donnadieu, B. Chaudret, H.A. el Makarim, J.-C. Barthelat, S. Ulrich, H.-H. Limbach, C. Moïse, New J. Chem. 25 (2001) 55.
[132] U. Schubert, Adv. Organomet. Chem. 30 (1990) 151.
[133] U. Schubert, in: B. Marciniec, J. Chojnowski (Eds.), Advances in Organosilicon Chemistry, Gordon and Breach, Yverdon-les Bains, Switzerland, 1994.
[134] J.Y. Corey, J. Braddock-Wilking, Chem. Rev. 99 (1999) 175.
[135] R.H. Crabtree, Angew. Chem. Int. Ed. Engl. 32 (1993) 89.
[136] J. Schneider, Angew. Chem. Int. Ed. Engl. 35 (1996) 1068.
[137] X.-L. Luo, G.J. Kubas, C.J. Burns, J.C. Bryan, C.J. Unkefer, J. Am. Chem. Soc. 117 (1995) 1159.
[138] K. Hussein, C.J. Marsden, J.-C. Barthelat, V. Rodriguez, S. Conjero, S. Sabo-Etienne, B. Donnadieu, B. Chaudret, Chem. Commun. (1999) 1315.
[139] F. Carre, E. Colomer, R.J.P. Corriu, A. Vioux, Organometallics 3 (1984) 1272.
[140] D.L. Lichtenberger, A. Rai-Chaudhuri, J. Chem. Soc. Dalton Trans. (1990) 2161.
[141] C. Aitken, J.F. Harrod, A. Malek, E. Samuel, J. Organomet. Chem. 349 (1988) 285.
[142] J.L. Huhmann-Vincent, B.J. Scott, G.J. Kubas, unpublished results.
[143] U. Schubert, E.K. Kunz, B. Harkers, J. Willnecker, J. Meyer, J. Am. Chem. Soc. 111 (1989) 2572.
[144] B. Beagley, K. McAloon, J.M. Freeman, Acta Crystallogr. Sect. B 30 (1974) 444.
[145] J.R. Moss, W.A.G. Graham, J. Organomet. Chem. 18 (1969) P24.
[146] H. Piana, U. Kirchgaessner, U. Schubert, Chem. Ber. 124 (1991) 743.
[147] A. Khaleel, K.J. Klabunde, Inorg. Chem. 35 (1996) 3223.
[148] (a) L. Carleton, Inorg. Chem. 39 (2000) 4510;
(b) L. Carleton, R. Weber, D.C. Levendis, Inorg. Chem. 37 (1998) 1264.
[149] (a) U. Schubert, K. Ackermann, B. Worle, J. Am. Chem. Soc. 104 (1982) 7378;
(b) U. Schubert, G. Scholz, J. Muller, K. Ackermann, B. Worle, R.F.D. Stansfield, J. Organomet. Chem. 306 (1986) 303.
[150] H. Rabaa, J.-Y. Saillard, U.J. Schubert, Organomet. Chem. 330 (1987) 397.

[151] D.L. Lichtenberger, A. Rai-Chaudhuri, R.H. Hogan, in: T.P. Fehlner (Ed.), Inorganometallic Chemistry, Plenum Press, New York, 1992.
[152] D.L. Lichtenberger, A. Rai-Chaudhuri, J. Am. Chem. Soc. 111 (1989) 3583.
[153] D.L. Lichtenberger, A. Rai-Chaudhuri, Organometallics 9 (1990) 1686.
[154] (a) A.J. Hart-Davis, W.A.G. Graham, J. Am. Chem. Soc. 93 (1971) 4388;
(b) H. Yang, M.C. Asplund, K.T. Kotz, M.J. Wilkens, H. Frei, C.B. Harris, J. Am. Chem. Soc. 120 (1998) 10154.
[155] X.-L. Luo, G.J. Kubas, J.C. Bryan, C.J. Burns, C.J. Unkefer, J. Am. Chem. Soc. 116 (1994) 10312.
[156] S. Zhang, G.R. Dobson, T.L. Brown, J. Am. Chem. Soc. 113 (1991) 6908.
[157] (a) M.-F. Fan, G. Jia, Z. Lin, J. Am. Chem. Soc. 118 (1996) 9915;
(b) S.-H. Choi, Z. Lin, J. Organomet. Chem. 608 (2000) 42;
(c) A. Lledos, G.J. Kubas, J. Huhmann-Vincent, unpublished results;
(d) I. Atheaux, B. Donnadieu, V. Rodriguez, S. Sabo-Etienne, B. Chaudret, K. Hussein, J.-C. Barthelet, J. Am. Chem. Soc. 122 (2000) 5664.
[158] M. Shimoi, S. Nagai, M. Ichikawa, Y. Kawano, K. Katoh, M. Uruichi, H. Ogino, J. Am. Chem. Soc. 121 (1999) 11704 (and references therein).
[159] J.F. Hartwig, S.R. DeGala, J. Am. Chem. Soc. 116 (1994) 3661.
[160] J.F. Hartwig, C.N. Muhoro, X. He, O. Eisenstein, R. Bosque, F. Maseras, J. Am. Chem. Soc. 118 (1996) 10936.
[161] C.N. Muhoro, J.F. Hartwig, Angew. Chem. Int. Ed. Engl. 36 (1997) 1510.
[162] C.N. Muhoro, X. He, J.F. Hartwig, J. Am. Chem. Soc. 121 (1999) 5033.
[163] I. Demachy, M.A. Esteruelas, Y. Jean, A. Lledos, F. Maseras, L.A. Oro, C. Valero, F. Volatron, J. Am. Chem. Soc. 118 (1996) 8388.
[164] W.H. Lam, Z. Lin, Organometallics 19 (2000) 2625.
[165] M.R. Smith, Prog. Inorg. Chem. 48 (1999) 505.
[166] S. Sakaki, S. Kai, S. Sugimoto, Organometallics 18 (1999) 4825.
[167] (a) K.W. Zilm, J.M. Millar, Adv. Magn. Opt. Reson. 15 (1990) 163;
(b) G.J. Kubas, C.J. Unkefer, B.I. Swanson, E. Fukushima, J. Am. Chem. Soc. 108 (1986) 7000.
[168] X.-L. Luo, G.J. Kubas, C.J. Burns, J. Eckert, Inorg. Chem. 33 (1994) 5219.
[169] (a) W.A. King, X.-L. Luo, B.L. Scott, G.J. Kubas, K.W. Zilm, J. Am. Chem. Soc. 118 (1996) 6782;
(b) X.-L. Luo, D. Michos, R.H. Crabtree, Organometallics 11 (1992) 237.
[170] G. Albertin, S. Antoniutti, S. Garcia-Fontan, R. Carballo, F. Padoan, J. Chem. Soc. Dalton Trans. (1998) 2071.
[171] E. Rocchini, A. Mezzetti, H. Rugger, U. Burckhardt, V. Gramlich, A.D. Zotto, P. Martinuzzi, P. Rigo, Inorg. Chem. 36 (1997) 711.
[172] (a) A.K. Burrell, J.C. Bryan, G.J. Kubas, J. Am. Chem. Soc. 116 (1994) 1575;
(b) M. Kohli, D.J. Lewis, R.L. Luck, J.V. Silverton, K. Sylla, Inorg. Chem. 33 (1994) 879.
[173] F.A. Cotton, R.L. Luck, Inorg. Chem. 30 (1991) 767.
[174] D.G. Gusev, D. Nietlispach, I.L. Eremenko, H. Berke, Inorg. Chem. 32 (1993) 3628.
[175] A. Mezzetti, A. Del Zotto, P. Rigo, E. Farnetti, J. Chem. Soc. Dalton Trans. (1991) 1525.
[176] B. Chin, A.J. Lough, R.H. Morris, C. Schweitzer, C. D'Agostino, Inorg. Chem. 33 (1994) 6278.
[177] E.P. Cappellani, P.A. Maltby, R.H. Morris, C.T. Schweitzer, M.R. Steele, Inorg. Chem. 28 (1989) 4437.
[178] N. Aebischer, U. Frey, A.E. Merbach, Chem. Commun. (1998) 2303.
[179] T.Y. Bartucz, A. Golombeck, A.J. Lough, P.A. Maltby, R.H. Morris, R. Ramachandran, M. Schlaf, Inorg. Chem. 37 (1998) 1555.
[180] (a) W.D. Harman, H. Taube, J. Am. Chem. Soc. 112 (1990) 2261;
(b) Z.-W. Li, H. Taube, J. Am. Chem. Soc. 113 (1991) 8946.
[181] (a) M.A. Esteruelas, E. Sola, L.A. Oro, U. Meyer, H. Werner, Angew. Chem. Int. Ed. Engl. 27 (1988) 1563;
(b) D.G. Gusev, A.B. Vymenits, V.I. Bakhmutov, Inorg. Chem. 31 (1992) 1.
[182] T.A. Luther, D.M. Heinekey, Inorg. Chem. 37 (1998) 127.
[183] A.A. Gonzalez, K. Zhang, S.L. Mukerjee, C.D. Hoff, G.R.K. Khalsa, G.J. Kubas, ACS Symposium Series, vol. 428, 1990, p. 133.